 CMES, vol.73, no.3, pp.209-266, 2011

ALE Formulation and Simulation Techniques in Integrated Computer Aided Design and Engineering System with Industrial Metal Forming Applications

A. Gakwaya[1], H. Sharifi[2], M. Guillot[1], M. Souli[3] and F. Erchiqui[4]

Abstract: A mechanical computer aided design and engineering system can be used to reduce the design-to-manufacture cycle time in metal forming process. Such a system could be built upon a solid modeling geometry engine and an efficient finite element (FE) solver. The maintenance of a high-quality mesh throughout the analysis is an essential feature of an efficient finite element simulation of large strain metal forming problems. In this paper, a mesh adaptation technique employing the Arbitrary Lagrangian-Eulerian formulation (ALE) is applied to some industrial metal forming problems. An ACIS boundary representation of the solid model is employed. This type of representation provides the necessary data for adaptive meshing techniques. To take care of large deformations, the Lagrangian types of mesh adaptation zones are used. The new mesh, which is updated at a given frequency, is found by iterating on the adaptation zones. During this process, mesh nodes are moved to new positions in order to have a more regular mesh size distribution. There are, however, cases where the ALE method needs an initial spatial mesh pattern to be able to complete the analysis. The required initial mesh depends on the plastic flow pattern of material. Examples of large strain metal forming problems illustrate the effectiveness of the method in industrial environment.

Keywords: arbitrary Lagrangian–Eulerian, ALE; adaptive meshing; virtual forging; large deformation; finite element; metal-forming; geometric modeling, ACIS.

1 Introduction

To reduce the manufacturing time and costs, an optimal process cycle is needed (Altintas 2007). Using powerful computers, long and costly traditional trial-and-

[1] Dept. of Mechanical Engineering, Laval University, QC, Canada, G1V 0A6
[2] School of Mechanical Engineering, Shiraz University, Shiraz, Iran
[3] LML, Boulevard Paul Langevin, Cité Scientifique, 59655 Villeneuve d'Asq Cedex, Lille, France
[4] Université du Québec en Abitibi-Témiscamingue, Rouyn-Noranda QC, Canada, J9X 5E4

error development processes are increasingly being replaced by numerical simulation methods. The finite element method (FEM) (Bathe, 1996; Belytschko 2000) is a class of numerical simulation tool that is widely used in the study of large deformation processes (Hamel 2000; Sheikh 2008; Groche 2007). This method has the ability to deal with geometrical complexities, nonlinear material properties, complex boundary conditions and so on (Rugonvi 2001; Stocker 1999). Using such a numerical simulation tool, for example in metal forming process, one can predict possible defects of the work-piece and possible failures of the tools before real testing. Different failure criteria can also be verified for the work-piece and for the tools in every stage of the forming process. The permanent deformation and the distribution of residual stresses at the end of the forming process can also be simulated. As a result, using finite element simulations, an interactive optimal process design can be performed.

Considering the cold forming process, which consist in forming a metal at temperature below its recrystallization level (for example at room temperature), the behaviour of the workpiece is related to its geometrical shape, material nonlinearities and applied boundary conditions. For integrated mechanical computer aided design and engineering (MCADE) process, a good solid modeling representation of the workpiece and toolings is needed to correctly handle the geometrical and boundary conditions complexities. Moreover, appropriate contact algorithms are required to handle the inter-components frictional interactions, and a suitable elastoplastic material model must be used to accurately reproduce the material behaviour. Since the results are mesh-dependent, a high-quality mesh should be maintained throughout the finite element analysis in order to insure convergence and correctness of the finite element results. As a result, a robust mesh updating algorithm must be used [Aquelet 2003; Longatte 2003, and 2009].

Mesh adaptation techniques based on the Arbitrary Lagrangian-Eulerian (ALE) formulation as described in (Askes 2004; Zohouri 2005) are now available in commercial FE codes [Halquist 2005] for both fluid and solid like problems. Here we are concerned with ALE application to some metal forming processes. The component geometric models use a solid boundary representation (BRep) technique of ACIS geometric engine. Such a representation is suitable for an ALE procedure as the data necessary for mesh updating can be obtained easily. Moreover, using BRep solid model makes visualization, verification, and interface to other packages easier. The ALE mesh can move independently of the material; however its topology, i.e. elements and connectivity, does not change during the adaptation and the solution variables on a deformed mesh are projected onto the new mesh. To deal with large deformations, the mesh adaptation zones of Lagrangian type have to be defined. And in these zones, the mesh is updated at a given frequency for each time

or deformation step of the process. The mesh nodes are moved to new positions in order to have a more regular mesh pattern. If the deformed object is considerably different from the original object, a spatial initial mesh pattern may however be required. The pattern of such an initial mesh is problem dependent and, as it is shown in one of the considered numerical examples, it depends on the material plastic flow pattern. In case the remeshing process is very difficult to perform, the problem can be solved using an Eulerian formulation on a fixed mesh [Aquelet 2006].

The objective of the paper is thus to evaluate an integrated MCADE-ALE formulation in the context of industrial application by considering an entire metal forming process running from CAD design through the FEA simulation for complex problems that require mesh adaptation or ALE remeshing algorithms. The paper is thus expected to provide, to designers and engineers in academia or industry, a better understanding of the different processes used to design and manufacture a part by cold forming. The first part of the paper thus describes the part and assembly design and meshing methodology using tools from a MCADE library. In the second part, the ALE conservative equations are described and an operator split method is used to solve the equations in an arbitrary moving mesh. Then examples illustrating both adaptive and non adaptive mesh applications are presented.

2 Parametric, feature-based solid-modeling of non-manifold geometries

Most of modern solid modeling packages either for design or analysis are based on parametric, feature-based 3D graphics packages that force the designer to use a bottom-up approach. However by using a design methodology that forces the user to think, at the outset, about the overall scope of the design and by requiring before hand from him to determine the features and their design intent, the design process can be systematically implemented in a top-down manner. The application of this methodology results in agile models that can easily be modified with changing design requirements. In a physical modeling based virtual manufacturing system, the geometrical models of the different interacting physical components are an essential ingredient around which all computer aided engineering activities are performed. The integration of material modeling, process simulation and computational mechanics are realized so that formed parts performance can be assessed by considering their complete material history. The used geometrical modeling approach is based on ACIS [ACIS 1] geometric engine implemented in ABAQUS/CAE software [Hibbit 2006]. This environment benefits from decoupling parametric specifications from geometrical ones. The choice of this ACIS development environment is very interesting since, in addition to the graphical services, it has the minimal geometrical functionalities necessary for the management of the names. This environment includes a set of reusable software components,

such as data management, visualization tools, geometric modeler, exchange interfaces, etc. Within the framework of the design of a model, two of the ACIS tools are mostly used, namely, the geometric numerical model and the visualization tool. The geometric numerical model is composed of classes of entities which make possible to create 2D and 3D objects. The two-dimensional objects can be created, either directly, e.g. circle by a center and a radius, or by constraints, e.g. circle tangent on two lines. ACIS makes it possible to build 3D geometric objects by revolution, extrusion, or Boolean operations. The underlying geometrical library is based on a Boundary representation (BRep) model, and offers mechanisms for visiting the internal structure of the objects. The geometrical core of ACIS engine implements a particular version of the boundary representation modeling. Indeed, contrary to the traditional BRep modeller, the data structure of ACIS has only downward references. The hierarchy of topological entities is described in Table 1 and a partial representation of a 3D solid example using this type of hierarchy is presented in Figure 1.

Table 1: Hierarchy of topological entities of the BRep structure of the ACIS core geometry.

Entity	**Definition**
Compound	Groups of topological entities.
Compsolid	Composite solid which is formed by a set of *solids* connected by their *faces*. It is the extension of the concept of *wire* and *Shell* to the solids.
Solid	Part of 3D space which is limited by connected *shells*.
Shell	Set of *faces* connected by their *edges*.
Face	Portion of a geometrical surface limited by a set of *wires*.
Wire	Set of *edges* connected by their *vertices*.
Edge	One dimensional topological entity, which corresponds to a curve generally limited by two *vertices*.
Vertex	Topological entity of dimension 0, which corresponds to a point.

The construction history is stored in each stage of a solid construction. An advantage of this type of data structure is its capacity to simply manage the cancellation of the last actions (undo). Indeed, to pass from a stage of construction i to a stage i–1, it is enough to return at the entrance of history point p_{i-1}, and to regenerate the geometry corresponding to this topological structure. There are no ascending links to manage. Based on this topological structure, ACIS proposes a set of functionalities to follow-up the history of the entities, in particular to the faces, in a

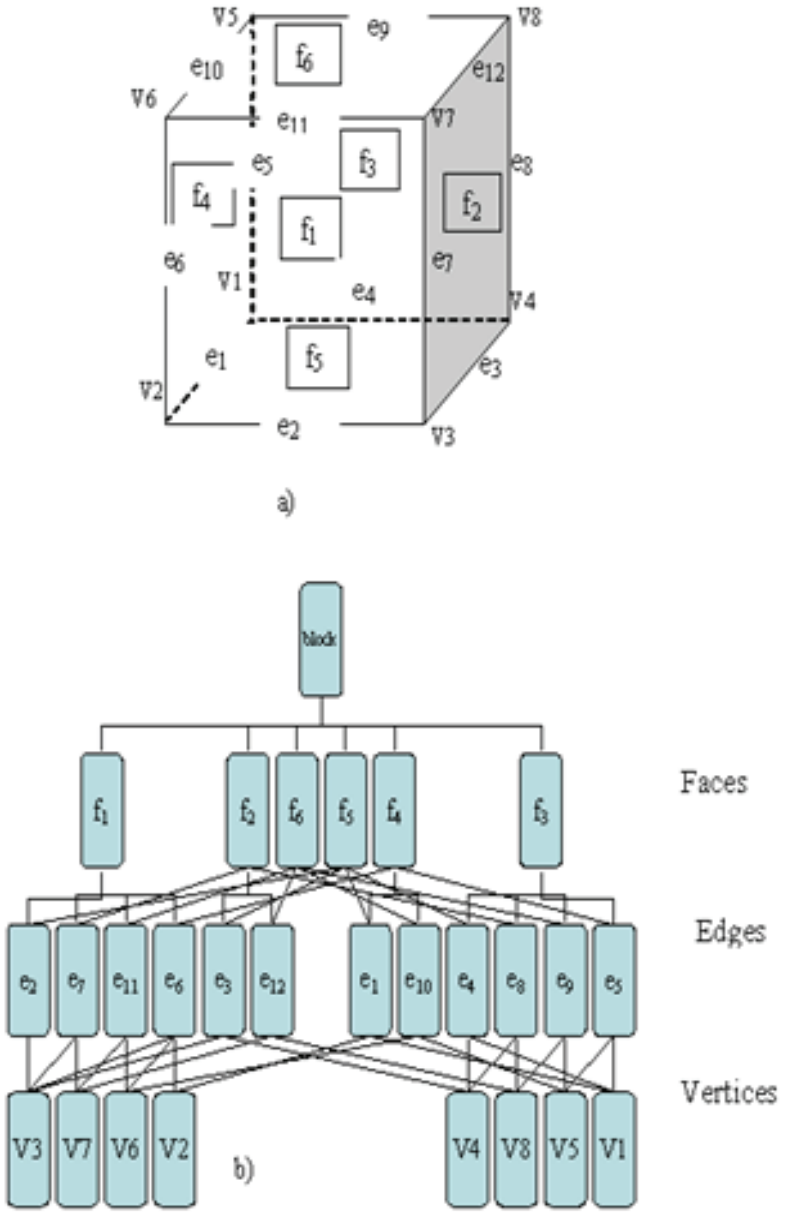

Figure 1: Representation of a block, a: The block geometry, b: BRep Structure.

construction operation. That enables us to trace and preserve, in the graph, the history of all the operations of construction of the parametric model. ACIS thus meets our needs for geometrical modeling (construction, search for information, etc), as well as management of topology (historical, exploration, etc).

2.1 Model attributes

Solid modelers have become common place in engineering departments in the last ten years due to faster PCs and competitive software pricing. They are the workhorse of machine designers. Solid modeling software creates a virtual 3D representation of components for design and analysis intents. Interface with the human operator is highly optimized and includes programmable macros, keyboard shortcuts and dynamic model manipulation. The ability to dynamically reorient the model, in real-time with 3D shading, is emphasized and helps the designer to maintain a 3D image.

A solid model generally consists of a group of features, added one at a time, until the model is completed. Engineering solid models are built mostly with sketcher-based features; 2D sketches that are swept along a path to become a 3D models. These may be cuts, extrudes or revolves. Design work on components is usually done within the context of a whole product using assembly modeling methods.

For inline design verification, several attributes are associated with a solid model. Each attribute defines a logical aspect of the model; for example, defining the geometry, defining material properties, and generating a mesh. In Abaqus/CAE environment, these attributes are associated to the model via different modules.

2.1.1 Part Module

A feature is an attribute of a solid model which represents the designer's intent and includes geometrical characteristics plus a collection of rules that administrate the behavior of the geometry. For example, an elliptical through cut is a feature, and the CAD software such as Abaqus/CAE must keep the diameters of the cut as well as the information that it must cut all the way through the solid. If you enlarge the size of the solid, the CAD software knows that the depth of the cut must be augmented so that it continues to pass through the solid. The Part module in Abaqus/CAE is used to create, edit, and manage the solid model. Abaqus/CAE stores each part in the form of a well-organized list of features. The parameters that define each feature combine to define the geometry of the solid. Figure 2 shows three parts of a simple metal forming simulation created by solids of revolution.

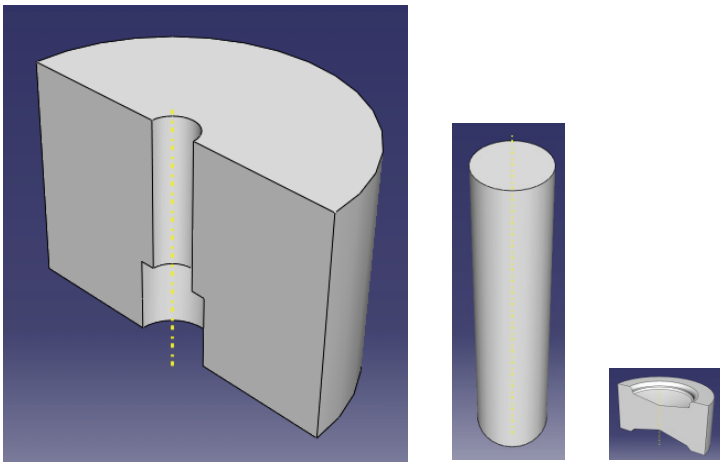

a) b) c)

Figure 2: Simplified metal forming parts a: die, b: punch, c: workpiece.

2.1.2 *Property module*

Material properties are another important attributes of a solid model. An appropriate material from a material library can be associated with a solid model. It is also possible to define and enter the material properties directly. Beside the material properties, in order to use the finite element analysis tool, material isotropic and anisotropic characteristics, solid sections such as, beam section and its orientation, shell section and its orientation, and so on, must be defined and assigned to the solid. Abaqus/CAE gives an interface in which the user can enter the material properties. The Property module of Abaqus/CAE software provides thus an interface to:

- define materials properties.
- define beam section profiles.
- define shell sections.
- assign sections, orientations, normal, and tangent to solid models.
- define composite layups.

- define a skin reinforcement.
- define inertia (point mass, rotary inertia, and heat capacitance) on a solid.
- define springs and dashpots between two points or between a point and ground.

All these attributes will be inherited by the finite element mesh entities.

2.1.3 Step module

To perform a FEA analysis, finite element modeling specifications such as: implicit or explicit solver, analysis time, solution accuracy tolerance, convergence criteria, and so on, must be defined. The Step module in Abaqus/CAE gives possibility to:

- Create analysis step: here a sequence of one or more analysis steps can be defined. The step sequence offers a handy way to simulate changes in the loading and boundary conditions of the model, changes in the interaction of the parts with one another, the elimination or addition of parts, and so on. Beside, steps permit to change the analysis procedure, the output data, and the possibility of various controls of the simulation procedure.
- Specify output requests. An output request describes which variables will be output during an analysis step, from which region of the model, and at what frequency they will be output.
- Specify adaptive meshing. Here, one can identify adaptive mesh regions and specify controls for adaptive meshing in those areas.
- Specify analysis controls, such as customizing general solution controls and solver controls.

2.1.4 Load module

Boundary conditions are another model attributes that must be specified for each step of analysis. They are step-dependent attributes as they can change from step to step. The Load module of Abaqus/CAE is used to define and manage the following prescribed conditions:

- Loads, either concentrated or distributed loading.
- Boundary conditions, either fixed, pivot, and so on.
- Predefined fields, for example initial velocity or initial stress field.

- Load cases, which are sets of loads and boundary conditions used to define a particular loading condition.

Complicated time or frequency dependencies load cases can also be defined in Abaqus/CAE.

2.1.5 Mesh module

Before any finite element analysis computation is started, the solid model must be subdivided into elements. Having an adequate mesh or grid is an essential part of any FEA analysis. A good CAD/FE software is able to generate a professional finite element mesh. Classical Mesh module offers various levels of mesh automation and control. The process of assigning mesh attributes to the solid model, such as seeds, mesh techniques, and element types is feature based. Therefore one can change the parameters that define a solid, and the mesh is regenerated automatically. Sometime it is necessary to simplify and/or partition complex geometry so that the CAD software recognizes basic shapes that it can use to generate a high-quality mesh. Most unpartitioned solid models are too complex to mesh by using pre-established mesh patterns. However, partitioning complex models into simple regions solve the problem. A Mesh module thus provides the following capabilities:

- Prescribing the mesh density at local and global levels.
- Model coloring that indicates the meshing technique assigned to each region.
- Several mesh controls, such as:
  - Element shape
  - Meshing technique
  - Meshing algorithm
  - Adaptive remeshing rule
- Verifying mesh quality.
- Mesh refinement procedures for improving the mesh quality.

3 ALE Adaptive Meshing

In large deformation problems, the final shape of the object can be considerably different from its original shape. A finite element mesh which is adequate at the

beginning of the finite element analysis can become unsuitable as the deformations become significant. These types of simulations can lead to severe element distortion and the analysis can be aborted because of occurrence of highly distorted elements. To continue the analysis, a remeshing procedure is thus highly needed. This is the case of most of bulk metal forming simulations and high velocity impact. Many authors worked for developing a suitable grid generation (Sharifi 1996) and remeshing techniques (Pavana 1998; Yazdani 1999).

Due to localized deformations, using an updated Lagrangian (UL) formulation for a stationary process is less attractive if a large number of remeshings is required. An adaptive meshing that does not alter the topology (elements and connectivity) of the mesh and maintains a topologically similar mesh throughout the analysis (i.e., elements are not created nor destroyed), often referred to as Arbitrary Lagrangian-Eulerian (ALE) analysis (Wisselink 2004), is now available in commercial FE codes [e.g. ABAQUS, LSDYNA]. This method combines the features of pure Lagrangian analysis (in which the mesh follows the material) and Eulerian analysis (in which the mesh is fixed spatially and the material flows through the mesh). The Arbitrary Lagrangian–Eulerian (ALE) formulation is now a standard approach in large strain solid mechanics to keep mesh distortion and element entanglement under control. The basic idea of the ALE formulation is the use of a referential domain for the description of motion, different from the material domain (Lagrangian description) and the spatial domain (Eulerian description). When compared to fluid dynamics, where the ALE formulation originated (Hughes 1981; Baaijens, 1993; Rekers 1995), the main difficulty of ALE solid mechanics is the path–dependent behavior of plasticity models (Gadala 2004). The relative motion between the mesh and the material must be accounted for in the treatment of the constitutive equation (Dvorkin 1993; van der Helm 1998). A fully automatic remeshing method is needed for the simulation of complex metal forming process (Rachik 2002) and high impact problems (Zhu 1997).

3.1 ALE formulation

3.1.1 ALE kinematics

Arbitrary Lagrangian Eulerian formulation, or the ALE method, is a time discretization method similar to the updated Lagrangian method. Both the motion of the mesh and the material motion must be described (Schreurs 1986). In Lagrangian formulation, the motion of matter is described by the mapping:

$$x = \varphi(X,t)x = \varphi(X,t) \tag{1}$$

where $\varphi(X,t)$ transform a body from the initial configuration onto the current (spatial) configuration. In an ALE formulation, the nodes of the discretisation can

move in space independently of the material, hence a third computational domain is needed. This domain is commonly known as the reference domain $\hat{\Omega}$ (or ALE domain). The mesh motion can be described by:

$$x = \hat{\varphi}(\chi,t)x = \hat{\varphi}(\chi,t) \tag{2}$$

So during the transformation $\hat{\varphi}$, points χ of the ALE domain $\hat{\Omega}$ are transformed into points x of the spatial domain. The three computational domains are depicted in Figure 3, together with their respective mappings.

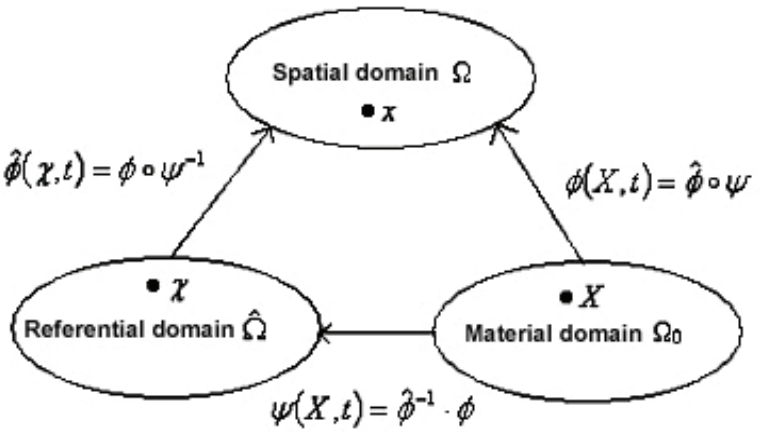

Figure 3: Correspondence between material, referential and spatial domains.

The initial values of particles position are given by the referential or ALE coordinates:

$$\chi = \varphi(X,0) \tag{3}$$

i.e. the coordinate χ_{ref} is labeled with the spatial coordinates x_{ref} at the beginning of the time step. At the end of each time step the referential situation is updated with the current situation. In contrast to the updated Lagrangian method, the referential coordinate χ_{ref} is not connected to the material points during a time step, but is connected to the grid points that move with the mesh velocity. If the referential configuration is the initial configuration we have a Total ALE description and if the

referential configuration is taken as the updated configuration of the updated Lagrangian scheme, we have an updated ALE approach which is the ALE formulation used herein.

A relation between the ALE coordinates and the material coordinates can be obtained through the following one-to-one composition mappings:

$$\chi = \hat{\varphi}^{-1}(x,t) = \hat{\varphi}^{-1}(\varphi(X,t),t) = \psi(X,t)$$

or

$$\psi = \hat{\phi}^{-1} \circ \phi \tag{4}$$

The material motion can thus be described by the composition of the grid motion and the ψ transformation:

$$x = \phi(X,t) = \hat{\phi}(\psi(X,t),t)$$

or

$$\phi = \hat{\phi} \circ \psi \tag{5}$$

As a result, the mappings onto the spatial domain and the material domain are functions of time, which means that a referential point corresponds at each time to a different spatial point and a different material point. In ALE algorithm, one prescribes or computes the mesh motion. Hence the material motion can be reconstructed from composition (5) if mapψ is invertible. The grid mesh displacement $\hat{u}$ and material displacement u are defined by following relations:

$$\hat{u}(\chi,t) = x - \chi = \hat{\varphi}(\chi,t) - \chi, u = x - X \tag{6}$$

relations which are almost identical except that in grid displacement, material coordinates have been replaced by ALE coordinates.

The material velocity v and the grid velocity $\hat{v}$ are respectively given by a material derivative following a material particle X or a grid particle χ:

$$v = \left.\frac{\partial \phi(X,t)}{\partial t}\right|_X; \quad \hat{v}(\chi,t) = \frac{\partial \hat{\phi}(\chi,t)}{\partial t} = \left.\frac{\partial \hat{\phi}}{\partial t}\right|_\chi = \hat{\phi}_{,t[\chi]} \tag{7}$$

The introduction of the referential domain has two important implications: (i) the nodal positions are introduced as unknowns and they must be solved for, and (ii) time updates, if present, change when a Lagrangian description is rewritten into

an ALE description. This last issue is treated in details in classical references on ALE techniques (Hughes 1981, Donea 1983, Belytschko 2000) and the resulting equation is given simply as

$$\frac{Df}{Dt} = f_{,t[\chi]} + \frac{\partial f}{\partial x_j}\frac{\partial x_j}{\partial \chi_i}\left.\frac{\partial \chi_i}{\partial t}\right|_{[X]} = f_{,t[\chi]} + f_{,j}\frac{\partial x_j}{\partial \chi_i}w_i = f_{,t[\chi]} + f_{,j}c_j \tag{8}$$

where f is any physical property and w_i is the referential grid particle velocity defined by:

$$w_i = \frac{\partial \psi_i(X,t)}{\partial t} = \left.\frac{\partial \chi_i}{\partial t}\right|_{[X]} \tag{9}$$

and c is the convective velocity defined as the difference between material and grid velocities:

$$c_i = v_i - \hat{v}_i = \frac{\partial x_i(\chi,t)}{\partial \chi_j}\left.\frac{\partial \chi_j(X,t)}{\partial t}\right|_{[X]} = \frac{\partial x_i(\chi,t)}{\partial \chi_j}w_j \tag{10}$$

Now introducing a vector notation, equation (8) can be written as:

$$\frac{Df}{Dt} = f_{,t[\chi]} + cgrad(f) = f_{,t[\chi]} + c\nabla f \tag{11}$$

The notation $\left|_{[X_a]}\right.$ means 'keeping X_a fixed'. Thus, Eq.(8 or 11) should be understood as follows: the time derivative of$f$ in a Lagrangian context (i.e. keeping X fixed) equals the time derivative of f in an ALE context (i.e. keeping χ fixed) plus the contribution of the convection; this convective contribution is proportional to the convective velocity c and to the spatial gradient of f [Askes, 2004].

The material time derivative of an arbitrary quantity f thus depends on the reference coordinates in which it is written. A convective term appears when f is not written as a function of the material coordinates. The spatial time derivative vanishes for stationary processes.

3.1.2 ALE continuity and balance of momentum equation

In ALE formulation both the mass and momentum balance equations are required. For the continuity equation, we have

$$\rho_{,t[\chi]} + \rho_{,j}c_j + \rho v_{j,j} = 0 \tag{12}$$

where a convective term appears due to the relative velocity between material and mesh velocity. For the momentum equation we have

$$\frac{\partial \sigma_{ij}}{\partial x_j} + b_i = \rho\left(\left.\frac{\partial v_i}{\partial t}\right|_{\chi} + c_j\frac{\partial v_i}{\partial x_j}\right) \tag{13}$$

where σ_{ij} is the Cauchy stress tensor and b_i is the body force vector per unit volume. The right-hand side expresses the inertia force with density ρ and material velocity v_i. When the ALE formulation is used, the weak form of the continuity and momentum equation then become respectively:

$$\int_\Omega \delta\tilde{p}\rho_{,t[\chi]}d\Omega + \int_\Omega \delta\tilde{p}c_i\rho_{,i}d\Omega + \int_\Omega \delta\tilde{p}\rho v_{i,i}d\Omega = 0 \tag{14}$$

(with $\delta\tilde{p} \in C^0$ being the weighting function),

$$\int_\Omega \delta\tilde{v}_i\rho v_{i,t[\chi]}d\Omega + \int_\Omega \delta\tilde{v}_i\rho c_j v_{i,j}d\Omega = -\int_\Omega \delta\tilde{v}_{i,j}\sigma_{ij}d\Omega + \int_\Omega \delta\tilde{v}_i b_i d\Omega + \int_{\Gamma t} \delta\tilde{v}_i\bar{t}_i d\Gamma \tag{15}$$

(with $\delta\tilde{v} \in C^1$ being the weighting function). If body and inertia forces are neglected, the weak form with the weight function δv reads as:

$$\int_V (\delta v \overleftarrow{\nabla}) : \sigma dV = \int_S \delta v.t dS_t \tag{16}$$

Then for hypo-elastic formulation, the rate of the weak form will be used so that the complete rate of the weak form of the ALE equations, which contains the material velocity as well as the grid velocity, can be derived from Eq. (16) as shown in (Belytschko 2000; Wang 1997):

$$\begin{aligned}\int_V \delta v \overleftarrow{\nabla}: \left[-L_g.\sigma + \dot{\sigma} - (v_m - v_g).\vec{\nabla}\sigma + \sigma tr(L_g)\right] dV \\ = \int_S \delta v.\dot{t}dS - \int_S \delta v.\left[(v_m - v_g).\vec{\nabla}\sigma\right] ndS + \int_S \delta v.t \overset{*}{J} dS\end{aligned} \tag{17}$$

where Lg is the gradient of the grid velocity and $\overset{*}{J^S}$ is the grid derivative of the Jacobian. Lagrangian and Eulerian contributions are clearly identified.

3.1.3 Material constitutive models

We are concerned with ALE applications involving large strains and dissipative material behavior, so the constitutive update is written in an incremental (or rate) format and the time derivatives have to be rewritten by means of Eq. (8), leading in any case to convective terms. For metal forming, the constitutive laws of an hypoelastic model are used to model elastoplastic behavior [Ponthot, 2002] as

$$\hat{\sigma}^C_{ij} = H^c_{ijkl} D^C_{kl} \tag{18}$$

where $\hat{\sigma}^c_{ij}$ is the objective rate of Cauchy stress tensor, H^c_{ijkl} is the constitutive matrix and D^c_{kl} is the stretching tensor, all three evaluated in a corotational system. Since stress rate is required, the convective derivative (8) is written for the Cauchy stress tensor σ as

$$\left.\frac{\partial \sigma}{\partial t}\right|_{\chi} = \left.\frac{\partial \sigma}{\partial t}\right|_{X} - c_j \cdot \frac{\partial \sigma}{\partial x_j} \tag{19}$$

A transport algorithm for the state variables is thus required and eqn(19) will be objectively integrated using the final instantaneous rotation method. This method is incrementally objective (independent from rigid-body rotation) and it is consistent with material constitutive relations (Belytschko 2000).

3.2 ALE solution methods

3.2.1 Updated ALE approach

Here an updated -ALE approach is used meaning that Eulerian substep is carried out not after every iteration as in (Schreurs 1986) but at the end of the time step (Wisselink 2000). Since relation between the position of an integration point in the current configuration and its position in the initial configuration is lost, every time the mesh is moved, the state variables have to be transported (Rodrıguez-Ferran 2002). The objective of using ALE approaches being to avoid excessive mesh distortion, the quality of the mappings between the spatial, material and reference domain is an important concern. In an updated-ALE approach, the reference domain coincides with the material domain of the previous load step, the difference between the material domain and the reference domain will be relatively small compared to a total ALE approach; hence only the quality of the mapping between reference domain and spatial domain needs special care.

ALE formulation involves two sets of equations that have to be solved: the equations of Newtonian mechanics (such as equilibrium) and the mesh motion. Their respective unknowns (e.g. material and nodal displacements) appear in both sets of equations, so the equations are coupled and ALE is thus usually termed a coupled formulation. Although, the fully coupled ALE approach represents a true kinematic description in which material deformation is described relative to a moving reference configuration (Belytschko 2000, Gadala 2004), a survey of the ALE literature (Stoker, 1999; Wisselink 2004) shows however that the majority of ALE analyses are based on a computationally convenient staggered approach. The disadvantage of coupled-ALE schemes is that they lead to larger matrices than decoupled-ALE. However, with a proper linearisation, quadratic convergence of the Newton–Raphson solution algorithm can be maintained (Gadala 2004). The reduction of number of iterations may balance the increase of computer cost per iteration.

In the staggered approach, material deformation and convective effects are treated separately using an operator splitting technique. The main advantage of this technique over the fully coupled approach is the reduction in the cost of implementation of ALE into current Lagrangian codes as the Lagrangian step is unchanged and only the Eulerian step algorithm needs to be added. Moreover, the decoupling of the Lagrangian and Eulerian steps results in simpler equations to be solved and this offer more flexibility in defining the new grid, as the latter is determined after the Lagrangian step. The decoupled ALE method, also called operator split ALE, is also more efficient since the grid displacement and the convective increment are calculated only once per time step. This approach is better tailored to explicit dynamic codes and is used in ABAQUS and other commercial software such as LSDYNA, etc. (Reckers, 1995; Benson, 1989).

3.2.2 ALE Finite element discretization

Updated Lagrangian (UL) step.

This step is similar to the UL formulation where the calculations of the finite element method to achieve equilibrium are performed. The mesh is attached to the material (χ = X), consequently convective effects are neglected ($c_j = 0$) and equation (15) reduces to

$$\int_{\Omega} \delta\tilde{v}_i \rho v_{i,t[\chi]} d\Omega = -\int_{\Omega} \delta\tilde{v}_{i,j}\sigma_{ij} d\Omega + \int_{\Omega} \delta\tilde{v}_i b_i d\Omega + \int_{\Gamma t} \delta\tilde{v}_i \bar{t}_i d\Gamma \tag{20}$$

In Equation (20), Ω is the current domain that follows the body and $\bar{t}$ is the prescribed traction boundary. v_i represents the virtual velocity field in the body (Ω), required to be C^0 (continuous function) and $\delta\tilde{v} \in C^1$ is the weighting function. **b**, **t** are the prescribed body force and traction vectors, respectively. σ is the Cauchy stress tensor, required to be C^1 (continuous function and first derivative). ρ is the material density and prefix δ designates an arbitrary, virtual and compatible variation. After finite element discretization of the body, virtual nodal displacements are eliminated and Equation (20) can be rewritten as the set of non-linear ordinary differential equations

$$M\ddot{X} + F^{int} - F^{ext} = 0 \tag{21}$$

where F^{int} and F^{ext} represent, respectively, internal and external force vectors acting on the finite element nodes, $\ddot{X}$ is the nodal acceleration vector and M, as obtained from the second term of (20), is the consistent mass matrix. For dynamic problems, Equation (21) is solved employing the explicit Central Difference method (Belyschko 2000). For quasi-static problems, inertia effects are neglected and the

first term of equation (21) disappears and it yields

$$F^{int} = F^{ext} \tag{22}$$

In a staggered ALE scheme, at each time step, this ALE technique is used to solve eqn 13 and the ALE operator is split in two steps: UL step and Eulerian step. The most accurate option is to first carry out a Lagrangian substep (mesh motion is neglected and the usual (Lagrangian) equations of mechanics are solved), followed by an Eulerian substep (to determine the mesh motion and to account for the convective terms (Reckers, 1995).

For quasi-static problems, a linearization of equation 21 lead to:

$$[K_m]\{\Delta u_m\} = \{\Delta F_{ext}\} \tag{23}$$

indicating that, in the predictor part, eqn 23 can be used to calculate only the material displacement. Then in the corrector part, only the material increment of the state variables ξ is integrated in time:

$$\xi^L = \xi^0 + \int_t^{t+\Delta t} \dot{\xi}\, dt \tag{24}$$

The predictor and corrector are repeated until equilibrium is satisfied.

Eulerian step

When equilibrium is achieved in the UL step, i.e. once the material displacement and the state variables after the Lagrangian ξ^L step are known, the grid displacement is determined using the material displacement and the new values of the state variables. Finally, the state variables at the integration points of the new grid ξ^{n+1} at t^{n+1} have to be calculated from the values ξ^L in the integration points of the old grid, also at t^{n+1}. This is an interpolation problem as no time change is involved, but it can also be written as a convection problem:

$$\xi^{n+1}(x_g^{n+1}) = \xi^L(x_m^{n+1} - \Delta u_c) \tag{25}$$

Since the mesh moves along with the material, the mesh obtained in this step is usually distorted. Therefore, the Eulerian step is performed by first applying mesh smoothing techniques to reduce mesh distortion and then by transferring data from the UL mesh (X) to the relocated mesh (χ).

A drawback of the decoupled method is that equilibrium is not checked at the end of the step. Equilibrium can be violated if the convection is not performed accurately. This leads to unbalance forces, which are carried as a load correction onto the next step. Large unbalance forces can lead to possible divergence.

3.3 Mesh motion techniques

3.3.1 ALE formulation implemented in ABAQUS [Hibbit et al 2006]

The framework for adaptive meshing in ABAQUS/Explicit is the Arbitrary Lagrangian-Eulerian method, which introduces advective terms into the momentum balance and mass conservation equations to account for independent mesh and material motion. There are two basic ways to solve these modified equations: (i) solve the non-symmetric system of equations directly, or (ii) decouple the Lagrangian (material) motion from the additional mesh motion using an operator split i.e. decoupled ALE formulation.

The operator split method is used in ABAQUS/Explicit because of its computational efficiency. Furthermore, this technique is appropriate in an explicit setting because small time increments limit the amount of motion within a single increment. First one define the ALE problem and then carry out its solution using an operator split methodology: (a) Use a Lagrangian step to advance the solution in time;(b) in Eulerian phase, first perform a mesh smoothing process and perform an advection sweep to remap the Lagrangian solution variable to the new mesh. Hence adaptive meshing in ABAQUS consists of two fundamental tasks: (i) creating a new mesh, and (ii) remapping solution variables from the old mesh to the new mesh with a process called advection. The remeshing step of the ALE method is characterised by the fact that the mesh topology remains unchanged. Therefore the remap problem reduces to the discretization of a convection problem. It is a linear convection problem, as the convective velocity vc is assumed to be known here.

3.3.2 Mesh smoothing methods in ABAQUS

The determination of the new mesh in ABAQUS/Explicit is based on four ingredients. Firstly, the calculation of the new mesh in ABAQUS/ Explicit is based on some combination of three basic smoothing methods: volume smoothing, Laplacian smoothing, and equipotential smoothing (smoothing methods are applied at each node in the adaptive mesh domain to determine the new location of the node based on the locations of surrounding nodes or elements). Volume smoothing relocates a node by computing a volume-weighted average of the element centers in the elements surrounding the node. Volume smoothing is very robust and is the default method in ABAQUS/Explicit. Laplacian smoothing relocates a node by calculating the average of the positions of each of the adjacent nodes connected by an element edge to the node in question. Equipotential smoothing is a higher-order method that relocates a node by calculating a higher-order, weighted average of the positions of the node's eight nearest neighbor nodes in two dimensions (or its eighteen nearest neighbor nodes in three dimensions). Secondly, the initial element gradation can

be maintained at the expense of element distortion if desired. Thirdly, optimal positioning of the nodes before the basic smoothing methods are applied can improve mesh quality and minimize the frequency of adaptive meshing required. Finally, solution-dependent meshing is used to concentrate mesh refinement near areas of evolving boundary curvature. It is possible to combine smoothing methods and geometric enhancements in order to help the user in specifying either a uniform mesh smoothing objective or a graded mesh smoothing objective.

During the smoothing step a new mesh is created at a specified frequency for each adaptive domain. The topology of the mesh, such as elements and connectivity, does not change during the adaptive procedures. No new elements are created and old deformed elements are not destroyed to improve the mesh quality. Empty elements cannot exist, so all elements have to be completely filled with material in each remeshing step. The new mesh is found by sweeping iteratively over the adaptive mesh domain and moving nodes to smooth the mesh. In the new mesh, the initial gradation of the original mesh can be preserved.

3.4 Data transfer technique in ABAQUS

As the mesh moves, solution variables are remapped to the new mesh. The methods used for advecting solution variables to the new mesh must be consistent, monotonic and second order accurate and conserve mass, momentum, and energy. Two approaches are applied to solve problem. In the first approach called convection approach, the grid time derivative is integrated in time. The second approach, the interpolation approach consists of two phases: in the Lagrangian phase the material time derivative is integrated in time and subsequently an interpolation step is performed in the so-called Eulerian phase. This is the approach used by ABAQUS and that is explained below. In an adaptive meshing increment the element formulations, boundary conditions, external loads, contact conditions, etc. are handled first in a manner consistent with a pure Lagrangian analysis. Once the Lagrangian motion is updated and mesh sweeps have been performed to find the new mesh, the solution variables are remapped by performing an advection sweep. The advection sweep accounts for the advective terms in the momentum balance and continuity equations.

3.4.1 Momentum advection

Nodal velocities are computed on a new mesh by first advecting momentum, then using the mass distribution on the new mesh to calculate the velocity field. Advecting momentum directly ensures that momentum is conserved properly in the adaptive mesh domain during remapping. Two methods are available for advecting momentum: the default element center projection method and the half-index

shift method (Benson, 1992). Both methods are applicable for all adaptive mesh applications. The element center projection method is the default method used to advect momentum and requires the fewest numerical operations. The half-index shift method is computationally more intensive than the element center projection method, but it may result in less wave dispersion for some problems.

3.4.2 Advection methods for element variables

Element and material state variables must be transferred from the old mesh to the new mesh in each advection sweep. Two methods are available for the advection of element variables: (i) the default second-order method based on the work of Van Leer (1977) and (ii) a first-order method based on donor cell differencing. Both advection methods incorporate the concept of upwinding and conserve the element variables in an integral sense when mapping from the old mesh to the new mesh (that is, the value of any solution variable integrated over the domain is unchanged by adaptive meshing). Using a conservative algorithm to advect the element density and the internal energy, automatically ensures conservation of mass and energy for an adaptive mesh domain without Eulerian boundary regions. Both advection methods are also monotonic and consistent. A method is monotonic if an element quantity with a monotonic, increasing spatial distribution over a portion of the old mesh remains as such in the new mesh. A method is consistent if, when solution variables are advected to a new mesh that is identical to the old mesh, all element quantities remain unchanged. Second-order advection is used by default for all adaptive mesh domains. It is recommended for all problems, ranging from quasi-static to transient dynamic shock. First-order advection is simple and computationally efficient; however, it tends to diffuse sharp gradients over time, especially in transient dynamic analyses or other problems that require fairly frequent adaptive meshing.

3.5 ALE Algorithm steps

The main steps of the ALE formulation are presented in following algorithm. First, in the initialization (A), all the data input is defined. Then, the time step looping of the ALE operator is performed in two steps: UL step (B.1) (where equilibrium is searched) and Eulerian step (B.2) (where nodal relocation and data transfer are done). Third in (C), data is evaluated for post-processing the results and the looping continues until final time is achieved.

Algorithm of the main steps of ALE formulation in an explicit FEM code

Phase A: Definition of the ALE model data
A1) Defining the ALE problem

- Define the domain of adaptive meshing.
- Chose the type of analysis (Lagrangian or Eulerian).
- Chose element types which must be first-order, reduced-integration, solid elements (4-node)

A2) Partition of the domain and detection of the geometric features

- Split the domain into multiple adaptive mesh domains if applicable
- Detection of geometric features, edges and corners.
- Activation or deactivation of geometric edges and corners of Lagrangian and sliding boundary regions.
- Application of shared edges rules.

A3) Mesh constraints

- Applying spatial mesh constraints to prescribe spatial mesh motion that is independent of the material motion.

Phase B: ALE operator *B.1: Use a Lagrangian UL step to advance the solution in time*
Time step looping: $t^{j+1} = t^j + \Delta t$
(B.1.1) for Dynamic case: solve (21) using the Central Difference method.
(B.1.2) Quasi-static case: solve (22) using the full Newton–Raphson method.

B.2: Eulerian step
B.2.1 Perform a smoothing process of the mesh

- Volume smoothing method.
- Laplacian smoothing method.
- Equipotential smoothing method.

B.2.2 Data transfer: remap the Lagrangian solution variables to the new mesh using an advection sweep using either a first-order advection or a second order advection sweep.
Phase C: Post processing and analysis termination

Figure 4. ALE Algorithm and solution process

3.6 Adaptive meshing techniques in metal forming process simulation

3.6.1 Defining adaptive mesh domains

Adaptive meshing is of great value in any problem where large deformation is anticipated because improved mesh quality can prevent the analysis from terminating as a result of severe mesh distortion. Adaptive meshing often provides faster, more accurate and more robust solutions than pure Lagrangian analyses. Adap-

tive meshing is particularly effective for simulations of metal-forming processes such as forging, extrusion, and rolling because these types of problems usually involve large amounts of non recoverable deformation. In ABAQUS (Hibbit 2006), adaptive meshing is performed in adaptive mesh domains, which can be either Lagrangian or Eulerian. Within either type of adaptive mesh domain, the mesh will move independently of the material. On the boundary of a Lagrangian domain, the mesh will follow the material in the direction normal to the boundary, so that the mesh covers the same material domain at all times. In metal forming, the adaptive mesh domains can be chosen to be one part, such as the workpiece or the die separately. So the part is a Lagrangian domain. In the process, the mesh moves as the shape of the part changes and will follow the metal flow directions. Eulerian adaptive mesh domains are usually used to analyze steady-state processes involving material flow. On certain user-defined boundaries of an Eulerian domain, material can flow into or out of the mesh. For example, in an extrusion case, the blank geometry is defined such that it closely approximates the shape corresponding to the steady-state solution: this geometry can be thought of as an "initial guess" to the solution. No special mesh is required for the steady-state case since minimal mesh motion is expected during the simulation.

3.6.2 Initial mesh design and initial smoothing

In metal forming, when a Lagrangian domain is used for adaptive meshing, the initial mesh design becomes very important in the simulation, because the topology of the mesh does not change throughout the analysis, while the shape of the workpiece may change dramatically during the cold forming process. We should predict the possible metal flow in the process and design a proper initial mesh which may allow the mesh to adjust automatically according to the direction of metal flow. This technique is sometimes critical for the success of adaptive meshing and it requires certain experience in the mesh design. We may see it in the application examples later. Initial mesh smoothing reduces the distortion of the initial mapped mesh by rounding out corners and easing sharp transitions before the analysis is performed. Therefore, it allows the best mesh to be used throughout the analysis (figures 5 and 6) (Ying et al., 2003).

3.6.3 Contact modeling

Cold forming process systems involve contact between workpiece and tools and between different tools as mentioned earlier. Contact itself is a typical nonlinear boundary condition in finite element analysis. The time changing contact conditions in cold forming because of large deformation of workpiece and the requirements of defect-free process sequence design make the problem even more compli-

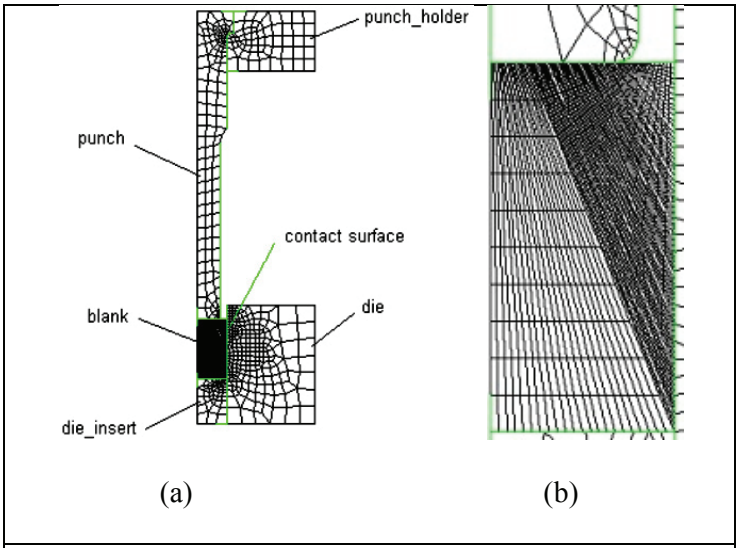

Figure 5: (a) Finite element model of the backward extrusion process, (b) Initial mesh of the blank

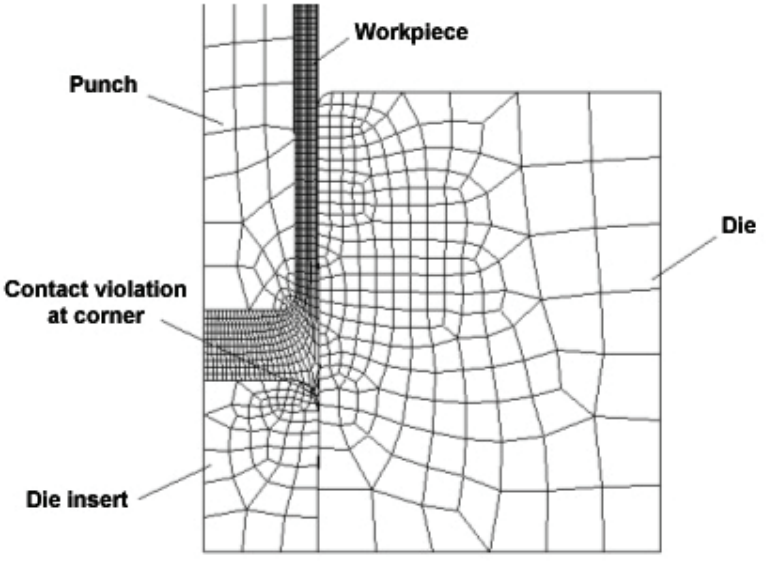

Figure 6: Contact violations at the corner

cated. How to model and solve the contact problem is one of the most challenging and difficult task in the process simulation.

In cold forming simulation, setting up a right contact interaction model, choosing proper contact formulations and algorithms are vital for the successful contact modeling. However, the formulations and algorithms provided by commercial softwares often have their limitations and are conditional in application. Contact elements are used to describe the contact between the bulk part and the tools. These elements are based on a penalty formulation and a Coulomb friction law is used. In application, only the isotropic friction models were used with the well-known Coulomb friction model characterized by the friction parameter η and available in standard fashion within the ABAQUS FEA code. Generally, the friction models are defined as a relation between the normal stress σ_n, the tangential stress τ_s and the relative tangential velocity V_S at the contact point between the part (deforming plastically) and the tool (supposed elastically deforming body). The tools are usually modeled as rigid in most forming simulation. However, in our applications the deformation of the tools was an important issue, especially for slender tools prone to buckling. This means that the deformation of the tools has to be taken into account if one wants to evaluate their durability (Vazquez et al, 2000; Lee and Im, 1999).

The proper determination of friction condition during metal forming operations is imperative for successful process design and production of parts. On Figure 6, the nodes on the lower right corner of the blank may easily slide along the contact surface between the insert and the die and cause penetration between the blank and insert when the deformation is large and the friction coefficient between blank surface and die surface is relatively small. This may be caused by the limitations of the contact algorithm. A possible solution is then to divide the die surface into two portions at the corner location and use a large friction coefficient between the blank outer surface and the lower inner surface of the die.

4 Numerical Applications

To demonstrate the robustness of the finite element simulation and the ALE method in metal forming process, three applications are presented in this section. We start with an example of tube hydroforming then we look at cold forming in a cup drawing process and, in the last examples, we consider an ALE application first (i) in a cold forming during a combined forward backward extrusion (virtual forging) and (ii) in a blanking operation where a seamless ring has to be cold formed by an integrated multistage multi-tool forming process.

4.1 Tube hydroforming application

This example of a multistage forming process is concerned with hydroforming of prebent tube and is provided in order to demonstrate the capability of ABAQUS in handling such kind of problems for idealized process and material parameters. A single non-adaptive mesh, obtained after a trial and errors process, was found to be suitable for this problem. A rotary draw bending process has been used for tube bending. The tube dimensions: D=68e-3 m, L=614e-3 m have been found by trial and error to compensate for the springback and make the bent tube fit into the hydroforming die. For the bend die model, the following parameters have been used: D=70.5e-3 m, bend angle (alpha) =180 degree; Dr=0.2 m; length of demi-tube section: 0.2 m. The clamp die model is a mirror of the semi-tube part of the bend die. Wiper shoe model has the following parameters: D=70.5e-3 m, alpha=360 degree; r=0.1 m (half of bend die). The tool design has been performed in ProEngineer and the parts have been exported in ABAQUS/CAE through IGS file. In ABAQUS, all tool parts are modeled as discrete rigid while the tube is modeled as deformable. The position and the movement of a rigid body have been defined by using a reference point. The bending tooling model and bend simulation results are presented respectively in Figure 7.

Material of the tube is an aluminum alloy with the following mechanical properties: density ρ =2700 kg/m^3; Young modulus E=73.1 GPa; Poisson's ratio $\upsilon = 0.3$; for elastoplastic behavior, simple elastic perfectly plastic material constitutive law has been used. (Yield stress $\sigma_y = 90MPa$;$\sigma_U = 124MPa$ at $\varepsilon_p = 0.3$). A friction coefficient of 0.15 has been considered for the interaction between the tools and the tube. Using ABAQUS explicit, both pressure loading and axial feeding have been applied for a successful completion of the forming process. After each intermediate step of the forming process, springback simulation has been performed using implicit analysis and the results carried forward to the next forming step as initial conditions. The tooling, finite element model and the results for pre-bent tube hydroforming are presented in figure 8.

4.2 Cup drawing process application

Part modeling: the cold forming process of cup drawing is studied in this application. First, in a geometric modeling step, one has to define the geometry of steel tools; i.e. die and punch geometry. Since they are assumed rigid and axisymmetric, only their profiles need to be defined. Then, the initial shape of cup workpiece model has to be created using geometry parameters obtained from a first cup forming; i.e. from a circular plate. The assembly of the three components at a certain step of the drawing process is presented in Figure 9. This figure shows an idealised geometry of the tools and the workpiece and the process at an intermediate time.

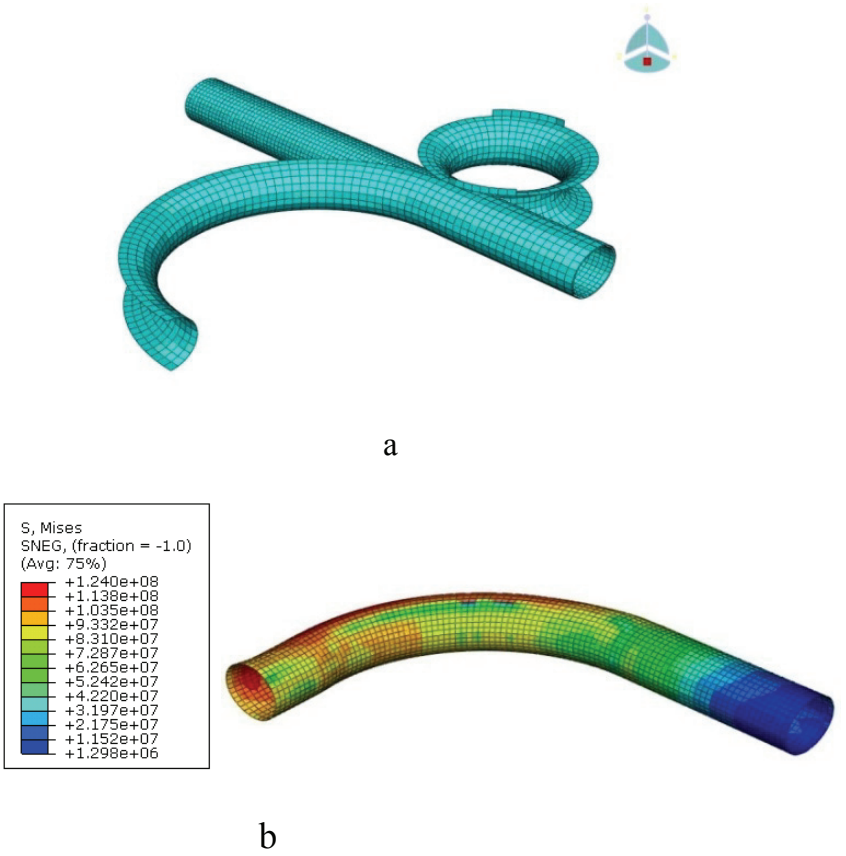

Figure 7: Tube bending tooling and simulation

Assuming an axisymetrical part, the workpiece CAD model can be defined from 8 segments or curves as indicated in Figure 10. Its dimensions are also shown in this figure. The cup drawing takes place during the passage of the workpiece between the die and the punch, and during which it undergoes radial and circumferential compressive forces. It will also be subjected to tension loads at the time of the exit from the die.

The forces on the punch are transmitted to the workpiece (cup) via the contact of the punch with the bottom of the cup or via the friction effects between the tools and the cup. As a result, the properties and the behaviour of the tool-workpiece interface are important parameters for the success of the operation. The material

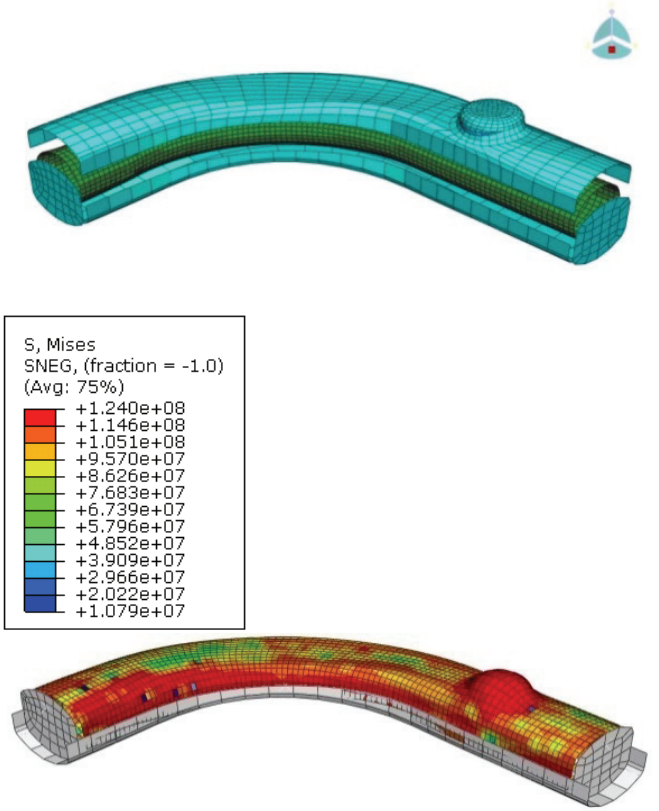

Figure 8: PreBent Tube Hydroforming Simulation

of the cup undergoes considerable plastic deformations during drawing. The tools are made of high strength steel, with mechanical properties that are considerably higher than those of the workpiece. So it is supposed that the tools undergo only elastic strain.

The general principal physical parameters of this type of process which must be considered are:

- Mechanical properties of the workpiece material: in function of deformations, rate of deformation and temperature;
- Friction of the workpiece-tool interface: in function of tool speed, contact

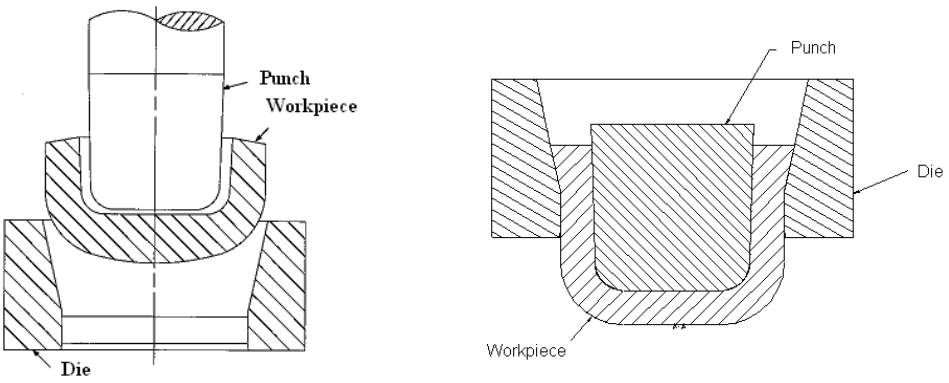

Figure 9: Cold forming of a cup and meshing

pressure of the process, type of the lubricant, temperature and surfaces finish.

- Thermal and mechanical efforts which cause small deformations in the tools.
- The plastic deformations work in the workpiece and the mechanical dissipation via friction generated heat which is assumed to be distributed uniformly in the workpiece and the tools.
- The non-symmetry of the workpiece before forming, the alignment errors between tools and the workpiece, or the anisotropic mechanical properties of the material.

The objective of this example is to show that when the deformation is not too severe, a good initial mesh can be used to run a successful analysis of the complete process using a standard updated Lagrangian formulation.

In our study, the following approximations were made to simplify the problem:

- The process is isothermal
- The mechanical properties of the material is independent of the rate of deformations
- The dynamic effects are negligible
- The solid has an axisymmetric geometry
- The material is isotropic

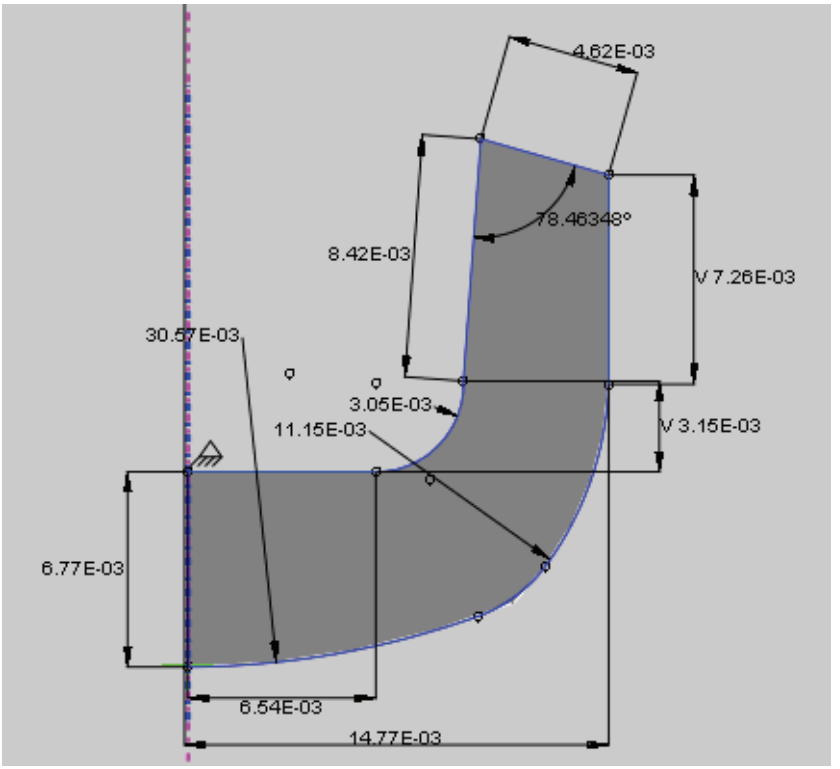

Figure 10: Principal nodes and dimensions of the initial cup workpiece.

Finite element analysis: Figure 11 shows the assembly before the drawing and an example of the grid mesh which has been used for the finite element analysis. Since it is assumed that the workpiece is axisymmetric, and that the tools are rigid, the analysis is done in 2D. The grid has 108 axisymmetric elements of the type CAX4R of ABAQUS library. This grid has 133 nodes. The frictional contact is modeled using the "surface to surface" contact option of the interaction module of ABAQUS. In the contact property, we have used a friction coefficient of 0.16 which was determined from our experiment.

The material of the cup has the following properties: Young modulus 39 GPA, Poisson's ratio 0.33, and the density of 2673 Kg/m^3. Figure 12 shows the plastic hardening behavior of this material using stress strain curve.

Since the goal of this application is to verify the stresses in the workpiece, the punch and the die are represented as a rigid body. In the Step module, we have created a general static step with a geometrical nonlinearity option and we have specified

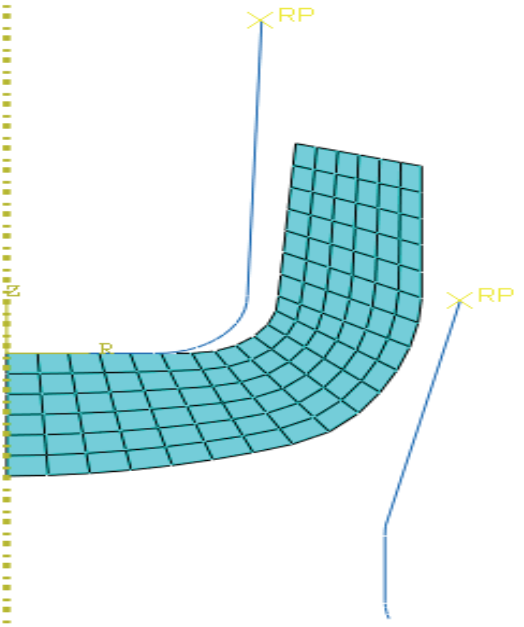

Figure 11: Mesh of the cup

150 as the maximum number of increments.

As boundary conditions, we have two options: either fix the punch using its reference point and move up the die so as to wrap the cup around the punch, or fix the die using its reference point and move down the punch. The second case is considered here and we have applied a displacement of 28mm in the negative vertical direction of the punch for the total time of the process. The punch is fixed in two other directions. Two surface to surface contacts, between the punch and the workpiece and between die and the workpiece, are declared in interaction module.

It is clear from Figure 13 that the finite element solutions converge to an acceptable solution. The deformations thus start in the corner, and then spread into the workpiece. The bottom of the workpiece does not have significant deformations, since it is always in blue. The maximum deformations were observed at the 87th increment and the registered maximum stress is approximately 31 MPa. In Figure 14 the strain energy versus the time increment is presented. The strain energy is high, between 20 and 60% of cold forming process, since during these increments, a great portion of the workpiece undergoes large deformations.

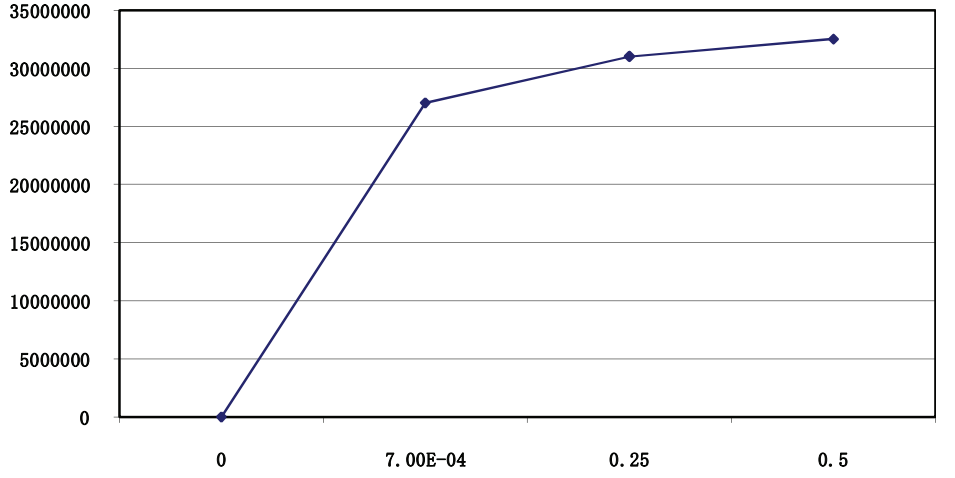

Figure 12: Material hardening curve (stress (Pa) versus plastic strain)

4.3 Virtual forging application: combined forward and backward extrusion

The objective of this example is to show that when the deformation is too severe, not only a good initial mesh is required but also an adaptive meshing strategy must be used in order to successfully run the simulation without numerical blow up. Here an ALE approach is used and good initial mesh is mandatory as it will be demonstrated at least for the used formulation.

Design of the cold forming process for a new mechanical part is not an easy task. Many tests and adjustments are often required to obtain satisfactory production conditions. Moreover, it is still difficult to ensure the quality of the product as a result of ductile facture, dimensional errors and failures of the tools caused by plastic deformation, wear, or low-cycle fatigue fracture (Skov-Hansen 1999). A typical system assembly of the cold forming process is shown in the Figure 15 (ASM 1969). The production system comprises a punch set (punch, punch holder, ...), a die set (die, die case, retainer, die insert, ...), a workpiece ejection system and the workpiece. A complete typical forming process often includes the following steps: (I) *Preloading*: for example in the tool assembly loading; (II) *Loading*: when the punch presses the workpiece and makes it deformed; and (III) *Unloading*: when the punch is removed and the workpiece is ejected. Usually in industrial applications, a simple stage of cold forming is not enough to obtain the desired final shape of the workpiece. Consequently, a multiple-stage forming process is often needed. Here,

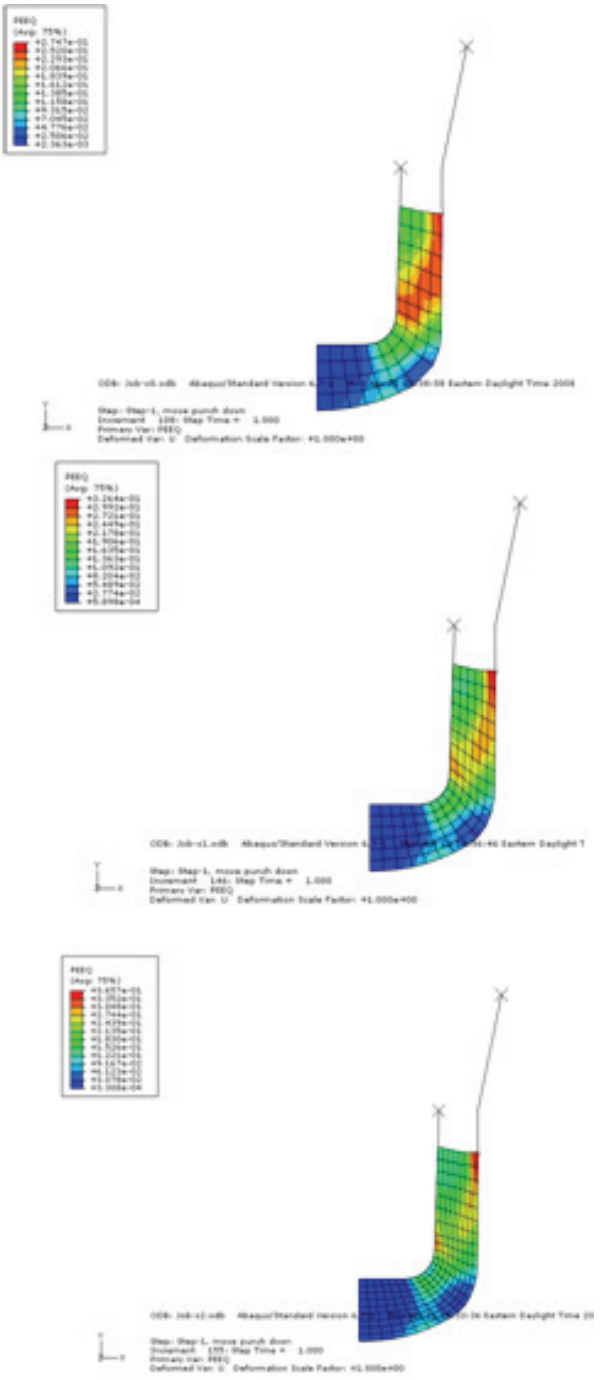

Figure 13: Plastic strain for coarse, intermediate and fine mesh

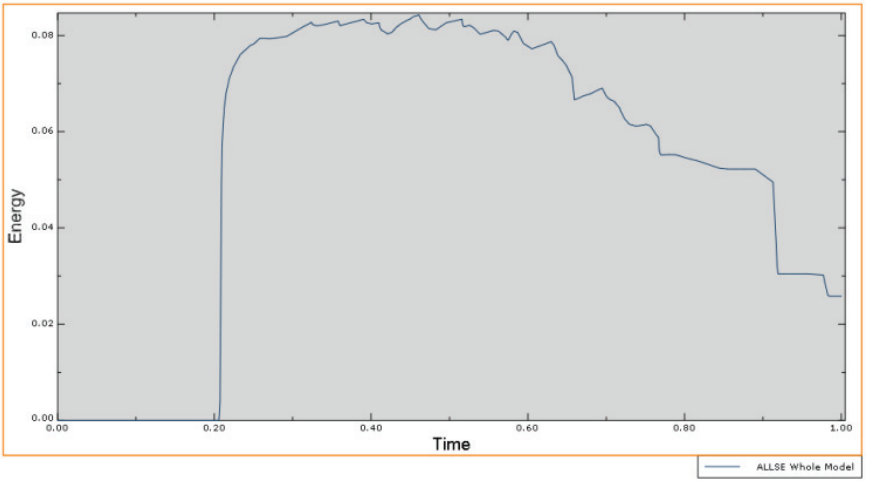

Figure 14: Total strain energy verses time

in each intermediate deformation stage, part of the total deformation is applied to the workpiece. Here we consider the case of combined forward backward extrusion process. The objective is to show that in case of important material flow, an initial adapted mesh is required for successful completion of ALE analysis. Since we are interested in the workpiece deformation and in the behaviour of the toolings directly connected to it, we simplified the system so that it can be illustrated as in Figure 16.

4.3.1 Geometry model and material properties

Assuming the axisymmetric feature of the system, we have thus presented it as an axisymmetric problem in ABAQUS. The CAD model of the simplified model is shown in Figure 16 and comprises:

- Workpiece: the blank, to be deformed to produce the final part, is a cylinder with a diameter equals to 1 inch and with height of 1 inch.
- Die: the matrix which is in form of a ring in which the workpiece is located; it makes possible to carry out the backward extrusion.
- Insert: the insert is in the form of a cylinder which supporting the workpiece, it makes possible to carry out forward extrusion.
- Punch: the punch is the tool which comes in contact with the workpiece and makes it deformed.

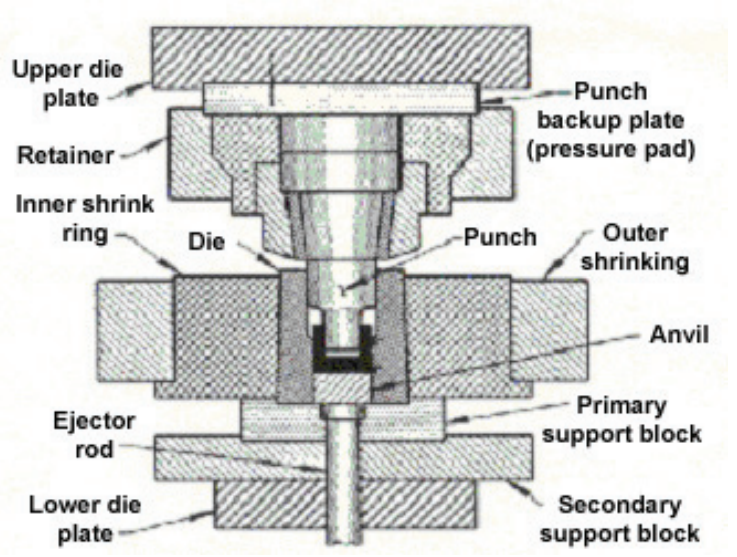

Figure 15: A typical system assembly of cold forming [ASM, 1969]

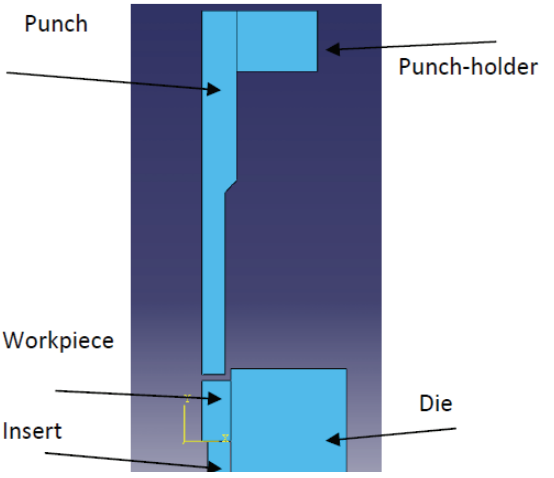

Figure 16: Simplified CAD model for forward-backward extrusion

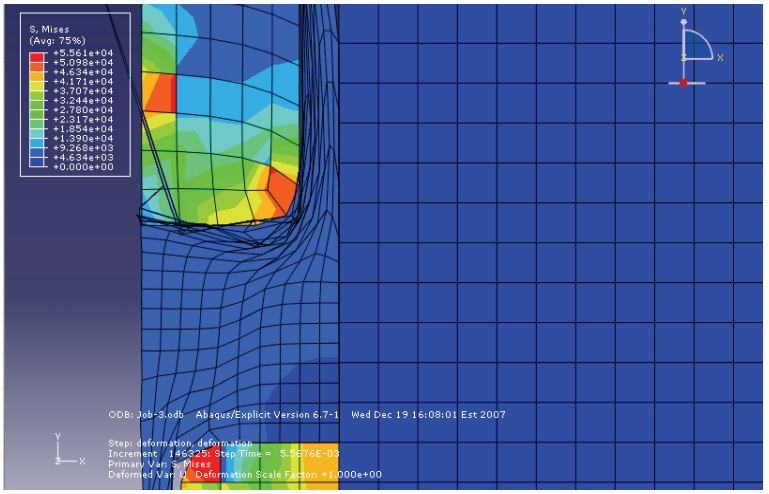

Figure 17: Results without ALE adaptive meshing algorithm

- Punch-holder: it is the support of punch. It guides the punch toward the workpiece.

4.3.2 Finite element modeling and analysis.

As a first try, we consider the case without using ALE adaptive remeshing algorithm. In such a case after a few steps, execution is aborted because of highly distorted element. Figure 17 shows the last result just before the execution is terminated. In the next step we use ALE adaptive meshing of ABAQUS without enforcing special initial mesh pattern. At the beginning it works well as it is shown in the Figure 18a. Unfortunately the execution also stopped after several steps, before reaching the final results, because of two excessively distorted elements. Figure 18b presents the results of such analysis just before the job abortion.

To overcome the above difficulty, we have introduced an initial mesh pattern, so that in a region where we anticipate more deformation we use a finer mesh. A suitable initial mesh configuration for this problem is presented in the Figure 19a. Using such an adapted initial mesh, the simulation has been successfully completed. The results of this simulation are shown in the Figure 19b.

The last example is concerned with a blanking operation where a seamless ring has to be formed by cold forming. The objective here is to study step by step, a multistage close die cold forming process simulation including unloading between intermediate steps. It is also desired to assess how the involved tooling costs (due to

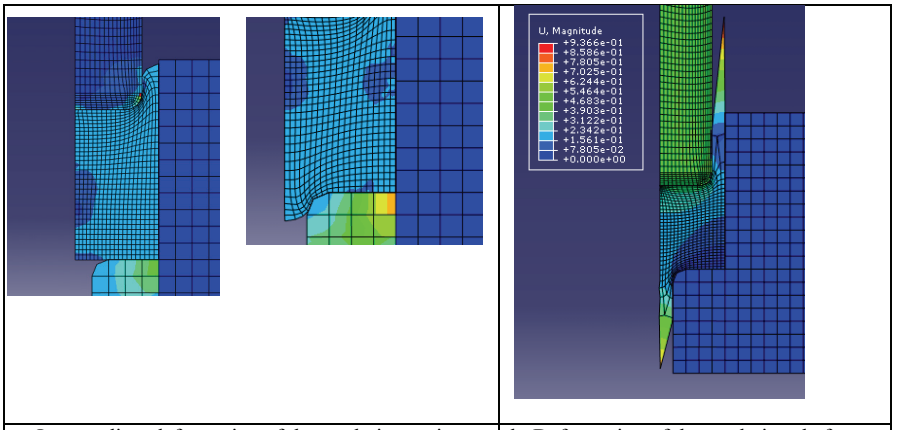

a: Intermediate deformation of the workpiece using pure ALE remeshing procedure.

b: Deformation of the workpiece before simulation is stopped, using pure ALE remeshing procedure.

Figure 18: Results with pure ALE adaptive meshing algorithm.

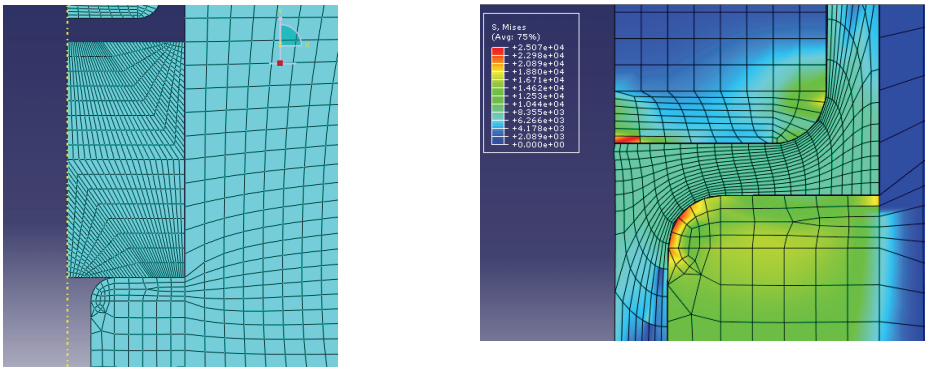

a) **b)**

Figure 19: Results with ALE adaptive meshing algorithm with adapted initial mesh

buckling failure) can be reduced through the use of a virtual metal forming system that avoids unnecessary physical prototyping. Due to the complexity of the physical model involving material damage evolution until final failure, most of the steps require mesh adaptation by rezoning technique, while the final step can only be accomplished through the use of a robust ALE based adaptive meshing with an

intermediate initial mesh redesign.

The complexity of the whole forming process involve preloading design, loading design during a forming step followed by unloading and springback calculation between two successive forming steps. Hence one has often to face data transferring between ABAQUS/Standard and ABAQUS/Explicit.

4.3.3 Parts geometry and material properties

The blank specimen is made of Stainless steel 304 with cylindrical shape characterized by 20.98 mm in diameter and 21 mm in length. Several tool sets are required for each forming step and typically a tool set comprises: upper punches, dies, die inserts, lower pins. As in application 3, we assume for simplicity axisymmetric components so that the geometric model is generated in the same way as in the preceding example. The difference being that here we have to generate and to assemble more components. M2 high speed steel material is used for all toolings. The material properties of the parts are show in the following tables 2 and 3.

Moreover, a ductile fracture model must be used in order to be able to simulate the final piercing stage and hence, one aim of this example is to evaluate the fracture model and porous material model used to represent the strength and deformation history of the part to be formed.

Ductile fracture simulation in ABAQUS: The ductile fracture criteria used in ABAQUS is based on Gurson's porous metal plasticity model [Gurson, 1977,] which assumes that the ductile fracture is caused by void nucleation and growth in material. The yield condition as modified by [Tvergaard, 1982] is:

$$\Phi = \left(\frac{q}{\sigma_y}\right)^2 + 2q_1 f^* \cosh\left(-q_2 \frac{3p}{2\sigma_y}\right) - (1 + q_3 f^{*2}) = 0 \tag{26}$$

where q_1, q_2, q_3 are material parameters. The function $f^*(f)$ models the rapid loss of stress carrying capacity that accompanies void coalescence. This function is defined in terms of the void volume fraction:

$$f^* = \begin{cases} f & \text{if } f \le f_c \\ f_c + \frac{\bar{f}_F - f_c}{f_F - f_c}(f - f_c) & \text{if } f_c < f < f_F \\ \bar{f}_F & \text{if } f \ge f_F \end{cases} \tag{27}$$

where

$$\bar{f}_F = \frac{q_1 + \sqrt{q_1^2 - q_3}}{q_3}$$

Table 2: Material properties of parts for close-die forming

Part name	Material type	Mass density (kg/m^3)	Young's Modulus (GPa)	Poisson's ratio	Yield stress (MPa)
Workpiece	Stainless steel 304	8000	196.948	0.3	289.579
All tools except Die case	M2 tool steel	8137	234.421	0.3	2344.217
Die case	H13 steel	7800	209.945	0.3	-

Table 3: Plasticity data of workpiece for close-die forming

True Stress (MPa)	True Plastic Strain
289.579	0.0
496.422	0.1
634.317	0.2
758.423	0.3
896.318	0.43
930.792	0.5
965.266	0.6
1048.003	0.8
1137.634	1.0
1206.582	1.25

In the above relationship, f_c is a critical value of the void volume fraction, and f_F is the value of void volume fraction at which there is a complete loss of stress carrying capacity in the material. The parameters f_c and f_F model the material failure when $f_c < f < f_F$, due to mechanisms such as micro fracture and void coalescence. These parameters are material data that can be obtained from experiment. When $f \geq f_F$ total failure at the material point occurs. $f = 0 (r = 1)$ implies that the material is fully dense, and the Gurson yield condition reduces to the Mises yield condition. $f = 1$ $(r = 0)$ implies that the material is completely voided, and has no stress carrying capacity. The model generally only gives physically reasonable results for $f < 0.1$ $(r > 0.9)$.

4.3.4 Blanking and piercing simulations in cold forming

For the ductile fracture process encountered in metal forming, studies are often concentrated on how to choose an appropriate ductile fracture criterion capable of precisely predicting its occurrence and how to optimize the process design to prevent the fracture [Pellet 2005; Kim,1999]. However in process like blanking and piercing during cold metal forming, the ductile fracture is an inherent feature, so things are quite a bit different [Ceretti 1997; Brokken 1998]. Not only is the initiation of fracture of concern but also the development of the crack and the shapes of the cutting edge and of the final chip are important.

Blanking or piercing is a shearing operation which involves elastic and plastic deformation and ductile fracture. The cutting surface after piercing contains four distinct zones as shown in Figure 20: rollover, shear zone, fracture zone, and burr. Depending on the material properties and punch-die clearance, secondary shear

may occur during material fracture. The rollover and the burr are results of the elastic and plastic deformations at the beginning of the blanking operation. An ideal part edge would have almost no rollover, burr, or fracture zone and exhibit almost 100% shear. However, the formation of the different zones is influenced by a number of parameters such as: material properties, punch-die clearance, tool wear, punch velocity and part geometry.

Finite element simulation can help process engineers to preview and thus get control of the shape of the blanking and piercing surface so as to assure the good quality of the products. However, for a successful simulation, several challenges in the FE simulation of blanking and piercing must be faced and adequately handled. These are:

1) to choose a proper ductile fracture criterion to predict precisely the initiation of ductile fracture,

2) to use a good material constitutive model to simulate the material behavior when plastic deformation and ductile fracture occur at the same time,

3) to use a proper algorithm to simulate the propagation of the crack in the finite element model,

4) to use a good remeshing technique to simulate the extremely large deformation during the process.

For the first challenge, one has to decide (important judgment) whether or not a criterion can take into account the cumulative deformation effect in the whole history of cold forming process. Moreover experiments are needed in order to get adequate material data of critical damage value. For the second challenge Gurson's porous metal plasticity seems to be a good solution. Metal softening effects due to voids nucleation and voids growth and the changes in yield condition are taken into account. This is the material model we used in our application. The ductile fracture criteria based on this theory are therefore advantageous from this point of view.

The correct prediction of the initiation of ductile fracture is realized by choosing correct ductile fracture criteria and the associated parameters. Here we use the porous metal failure criteria in ABAQUS. The f_F used here is 0.1, and the f_c used is 0.08. They are material parameters and can be determined by experiments.

Multi-stages forming processing: The whole forming process includes five stages. The first four stages are closed die forming. The fifth stage is piercing. In each stage the die is shrink fitted by the die case so that there are preloads in the die, the die insert and the die case. This is to strengthen the die. After the pressing is

finished, the punch is moved up and the workpiece is ejected by the knock-out pin, except in the last stage.

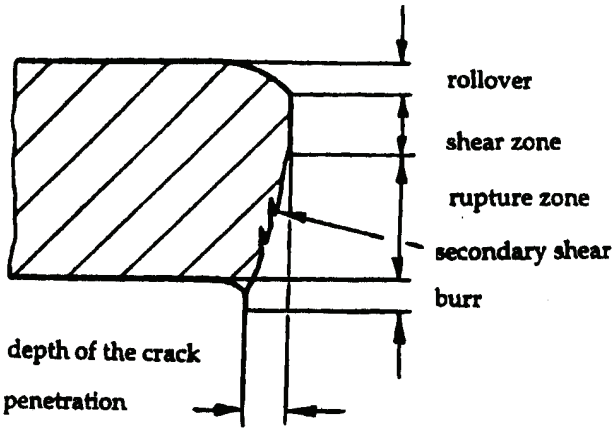

Figure 20: Shape of the cutting surface of blanking or piercing

4.3.5 FE modeling and interpretation:Element type

Since the process systems are assumed to be axisymmetric, we use axisymmetric solid element in all the five stages simulation to reduce the problem size. In all the FE models, 4-node quadrilateral reduced integration element (CAX4R) was used to simulate the workpiece and the tools except the die insert in the first stage (see Figure 16). The reasons are given in Application 1 [Ying 2003]. We use 6-node modified triangular elements (CAX6M) to simulate the 1st die insert as it has an arc edge and a sharp corner.

Material models The material model of the workpiece is an isotropic elasto-plasticity model with isotropic hardening. When the stress is below the yield stress the material is elastic. When the stress exceeds the yield stress, isotropic work hardening law is used and the material is hardened. The material models for the tools are assumed to behave elastically. But we gave a yield stress to check if the stress exceeds it. When this happens the material will become perfect-plastic and the tool fails.

Contact simulations Different contact algorithm are available in ABAQUS/Explicit, and care should be taken in choosing which one is most appropriate to a particular situation and to the contact parameters to be used. Below we illustrate typical

problems we encountered in our application of cold forming simulation using both balanced master-slave approach (supposed to be more precise) and pure master-slave approach. If there is a large density difference since the workpiece is usually much softer and more flexible than tools, we may have warning messages during the analysis indicating 'mass mismatching' in the contact pairs of workpiece surface and tool surface.

(i) When balanced contact algorithm is used and the deformation become large there will be contact noises at these areas or unrealistic deformation of tools. This is illustrated in Figure 21 that compare the deformation at the beginning and at the middle of this cold forming process and from which we can see that using balanced contact approach let the profiles A and B of the tools deformed unrealistically (encountered in ABAQUS 5.8). Hence a proper choice of contact parameter is an asset. This was fixed by letting the weight parameter to be zero to make pure master-slave contact formulation to work.

(ii) As for the pure master-slave formulation, we must be careful to select the slave and master surfaces correctly to achieve the best possible contact simulation. Some simple rules to follow are:
the slave surface should be the more finely meshed surface; and if the mesh densities are similar, the slave surface should be the surface with the softer underlying material.

Since tools are usually made of harder materials than the workpiece and large deformation of tools is not allowed for the sake of high quality requirements of product, we often use the tool surfaces as the master surfaces and the surfaces of the workpiece as the slave surfaces.

However by using pure M-S (master-slave) approach we still have master surface penetration problems in some situation. Figure 22 shows the same simulation example as in Figure 21 but using pure M-S approach. Penetration occurs at the contact corner. We can only make the mesh as fine as possible at this area and neglect the error. This is the limitation of the algorithm itself.

In the present application, all tools and workpiece are deformable and pure master-slave contact models are used. The contact sliding models used in all stages forming simulation are almost all finite sliding, except those in the first stage between the knock-out pin and the workpiece and between two tools and that are small sliding. In fact in our application small sliding doesn't show much of its advantage in time saving. On the contrary it may bring difficulties from time to time because of its limitation.

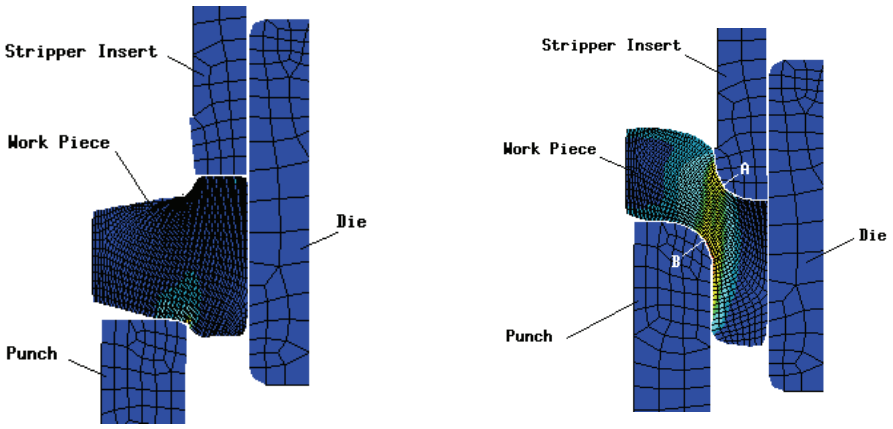

a) At the beginning of the process b) At middle of the process

Figure 21: Deformation of a cold forming system when using balanced approach

The friction models are simplified in all the stages of the forming process. The friction coefficients are supposed to be constant and independent of the slip rate and contact pressure. The friction coefficients between the workpiece and the tools were taken as 0.1 as suggested by books and papers on metal forming under good lubrication conditions [Lee 1996; Lange 1985]. The friction coefficients between two tools are given as 0.3, supposing that they are sticking to each other and the friction is severe. Here the friction influences are only symbolic.

Boundary conditions The die, die insert, ejection pin and die case are supported by a relatively stiff foundation, so the restrains in y direction are given to their bottom surface. ABAQUS does not automatically apply any boundary conditions to nodes located along the symmetry axis, so radial or x direction restrains are given to these nodes. Here we gave x symmetry plane restrains instead of zero displacement in x direction.

4.3.6 Process simulation

The five-stage closed die cold forming process is simulated stage by stage. Every stage includes shrink fits (preloading), pressing (loading), removing of punch and ejection of workpiece (unloading). The ejection of workpiece is simulated by moving down the die set instead of moving up ejection pin, since we don't want to

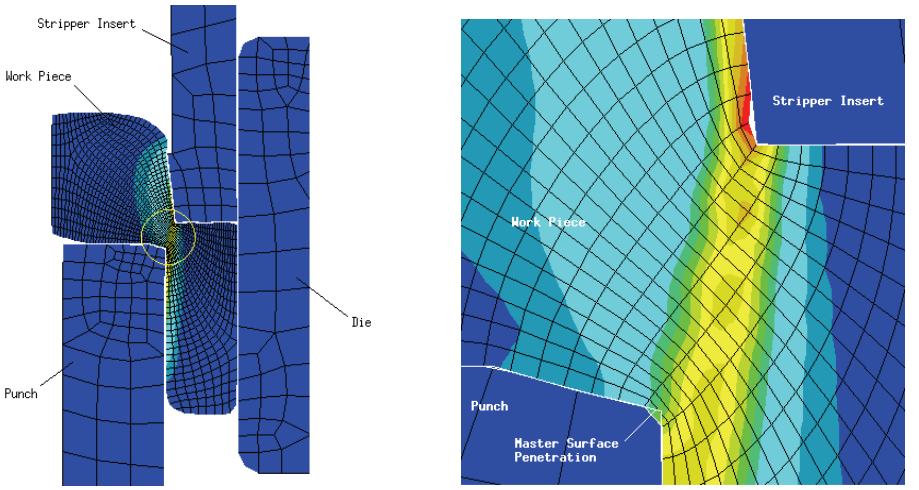

Figure 22: Deformation of a cold forming system when using pure M-S approach

change the position of the workpiece in our vision. The two procedures are equal as the relative motion between part are the same in these two situations.

The process simulation for each stage can be visualized continuously from preloading to ejection of the workpiece by animation, including the piercing stage. We can see clearly how the fracture initiated and propagated and how the piecing hole is formed, and finally how the chips are removed. And hence, the implementation of the 'virtual production' is illustrated to some extent.

A pseudo algorithm giving the main analysis steps used in the process simulation analysis is listed below (Table 4) where A/S and A/E stands for Abaqus Standard and Abaqus Explicit respectively.

Stage 1: from initial blank to first semi-finished product

Analysis 1: cdst11.inp A/S

STEP 1: SHRINK FIT BETWEEN DIE1 AND DIECASE1

STEP 2: MOVE PUNCH1 DOWN

STEP 3: MOVE PUNCH1 UP

STEP 4: MOVE DIE1 SET (DIE1, INSERT1, DIECASE1) DOWN

Analysis 2: cdst12.inp A/E OLD JOB= CDST11

STEP 5: TRANSFERING DATA OF BLANK FROM A/S TO A/E

Stage 2: from first semi-finished product to 2^{nd} semi-finished product

Analysis 3:cdst21.inp A/S OLD JOB= CDST12

STEP 6: SHRINK FIT BETWEEN DIE2 AND DIECASE2
Analysis 4: cdst22.inp A/E OLD JOB=CDST21
STEP 7: MOVE PUNCH2 DOWN
STEP 8: MOVE PUNCH2 UP
STEP 9: MOVE DIE2 SET(DIE2, INSERT2, DIECASE2) DOWN
Stage 3: from 2^{nd} semi-finished product to 3^{rd} semi-finished product
Analysis 5: cdst31.inp A/S OLD JOB= CDST22
STEP 10: SHRINK FIT BETWEEN DIE3 AND DIECASE3
Analysis 6: cdst32.inp A/E OLD JOB=CDST31
STEP 11: MOVE PUNCH3 DOWN
STEP 12: MOVE PUNCH3 UP
STEP 13: MOVE DIE3 SET (DIE3, INSERT3, DIECASE3) DOWN
Stage 4: from 3^{rd} semi-finished product to 4^{th} semi-finished product
Analysis 7: cdst41.inp A/S OLD JOB= CDST32
STEP 14: SHRINK FIT BETWEEN DIE4 AND DIECASE4
Analysis 8: cdst42.inp A/E OLD JOB=CDST41
STEP 15: MOVE PUNCH4 DOWN
STEP 16: MOVE PUNCH4UP
STEP 17: MOVE DIE4 SET (DIE4, INSERT4, DIECASE4) DOWN
Stage 5: final piercing operation from 4^{th} semi-finished product
Analysis 9: cdst511.inp A/S OLD JOB= CDST42
STEP 18: TRANSFERING DATA OF BLANK FROM A/E TO A/S
Analysis 10: cdst512.inp A/S OLD JOB= CDST511
STEP 1: REZONING OF BLANK (generate adapted initial mesh)
Analysis 11:cdst513.inp A/E OLD JOB= CDST512
STEP 2: TRANSFERING DATA OF BLANK FROM A/S TO A/E
Analysis 12: cdst514.inp A/S OLD JOB= CDST513
STEP 3: SHRINK FIT BETWEEN DIE5 AND DIECASE5
Analysis 13: cdst522.inp A/E OLD JOB= CDST514
STEP 4,5,6: MOVE PUNCH5 DOWN FOR PIERCING.

Table 4 Pseudo algorithm for the process simulation of a multistage-multiple tooling piercing operation

First stage forming and unloading

The 1^{st} punch is moved down 3.782 mm evenly in 2 seconds in the forming process and then is moved up 3.782 mm evenly in 1 second. At the beginning, the apex of the punch is just on the top of the blank. ABAQUS/Standard 5.8 was used to do the analysis, i.e. a pure Lagrangian formulation is used for this step. For the FE model, we used 4-node quadrilateral reduced integration element (CAX4R) to simulate the blank and the 1st punch, the 1st die, and the 1st lower pin. A 6-node modified triangular element (CAX6M) was used to simulate the 1st insert as it has an arc edge and a sharp corner. Contact problems are handled using pure master-slave algorithm. The contact interaction model between the 1st punch and work piece, and 1st knock out pin and work piece are small sliding. The contact interaction model between the 1st die and work piece, and 1st insert and work piece are finite sliding. All tools and work piece are deformable. The friction coefficient between the work piece and tools is supposed to be 0.08. The friction coefficients between two tool parts are 0.5. The analyses results are shown for shrink fit, loading and unloading operations for stage 1, but will not be repeated for the other stages.

Figure 23 gives the punch-stroke curve for the first stage. The maximum load is about 889.64 KN. Figure 24 gives the Von-Mises contour without shrink fit and the die case. It seems from the picture that the shrink fit helps to improve the stress state of the die, but it brings higher stress concentration on the die insert. Possible explanation could be that the shrink fit gives the die and die insert a preloading of compressive stress. In the pressing, a tensile stress is added to the die which lowers the stress. But for the die insert a compressive stress is added to some of the area of it and makes the stress even higher. So when adding shrink fit we should check the effects on all tool parts. FE process simulation enables the process engineer to check this.

From the above, we can notice that the unloading course will bring changes to the states of both the workpiece and the tools of the processing system as well as the loading course. So the simulation of unloading is as well important as the simulation of the loading course.

The stress here is the residual stress. The stress and the strain will be inputted to the next analysis step and become the initial stress and strain of the next forming stage. By this way the accumulated effects of stress and strain states of the workpiece in former stages of forming are taken into account into later stages of forming and allow the simulation results to become more near to the real situation.

Results analysis: From unloading analysis (Figure 24), it was observed that the most critical tool part is the first die. The residual stress is about half of the maximum value in the stroke. If we want to extend the life of the tool, we need to either

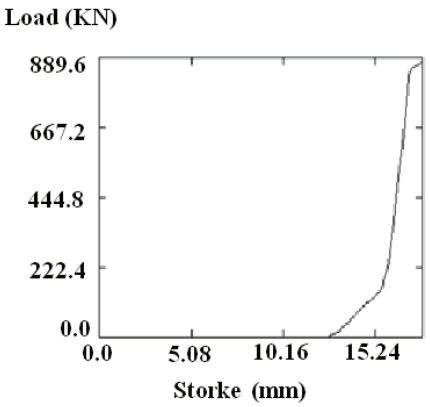

Figure 23: Punch load–stroke curve for the first stage

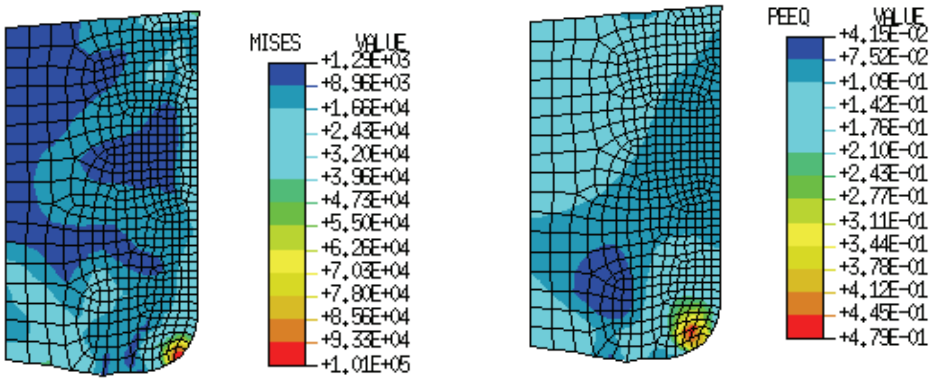

(a) (b)

Figure 24: Final (a) Von-Mises stress contour (in Psi Maximum is 696.3 MPa) and (b) Equivalent plastic strain contour after 1^{st} stage forming

use a good material or change the design to enhance it. At this stage the plastic strain is not large.

Second Stage Forming:

ABAQUS/Explicit 5.8 was used to do the analysis. The apex of the 2nd punch was moved down 7.05 mm (0.277599 inches) from the top of the deformed blank.

FE model for the second stage

As in first sage, we use 4-node quadrilateral reduced integration element (CAX4R) to simulate the blank and all the tools. Contact problems are handled using pure

master-slave algorithm. The contact interaction model between the 2nd punch and the workpiece, and 2nd knock out pin and workpiece and 2nd insert and work piece are small sliding. The contact interaction model between the 2nd die and workpiece are finite sliding. All tools and workpiece are deformable. The friction coefficient between the workpiece and tools is supposed to be 0.08. The friction coefficient between both tool parts is 0.5. An Arbitrary Lagrangian-Eulerian Formulation was used with an adaptive meshing domain corresponding to the workpiece and 2nd die model.

Results analysis:

From Figure 25 we can see that the most critical tool part is the 2nd die. If we want to extend the tool's life, we should change the design to enhance it. At this stage the plastic strain increased on the 1st stage level. So if we want to control the strain we must consider both two stages forming processes.

The second to the forth stages simulation

From the 2nd to the 4th stages, we use ABAQUS/Standard to simulate the shrink fits between dies and die cases and ABAQUS/Explicit to simulate the forming from loading to workpiece ejection. The data of the workpiece is transferred naturally from one analysis to another with the results of former forming simulation analysis to be used as initial stress and strain states in the latter forming simulation analysis. So the stress, strain and deformation effects are accumulated stage by stage similar to the real process situation. This is accomplished in Analysis 3 to Analysis 8 of Table 4.

In the three forming stages simulation when using ABAQUS/Explicit, the loading rate is accelerated in order to achieve efficient analysis while still keeping acceptable quasi-static solutions. Adaptive meshing is used in the workpiece to deal with the large deformation and mesh distortion.

The punches are all in high stress states in the 100% stroke but have not exceeded the yield stress yet. The equivalent plastic strain in the workpiece after the 2nd stage has an extremely large value near the bottom outer round corner.

Then we use A/S in the first stage for forming and unloading and only used A/E in the second forming stage.

2. The unloading simulates using A/E yields unacceptable results (the unloading process is static and residual stress must be accurately computed).

3. In the version of ABAQUS/Standard used to perform the 1st forming stage, we found contact problems between the work piece and the 1st die insert. Penetration happens when a small sliding formulation was used. The reason may be that the small sliding algorithm is not good enough for dealing with highly curved master surface, hence a solution was to use finite sliding model. Sometimes, the nodes on

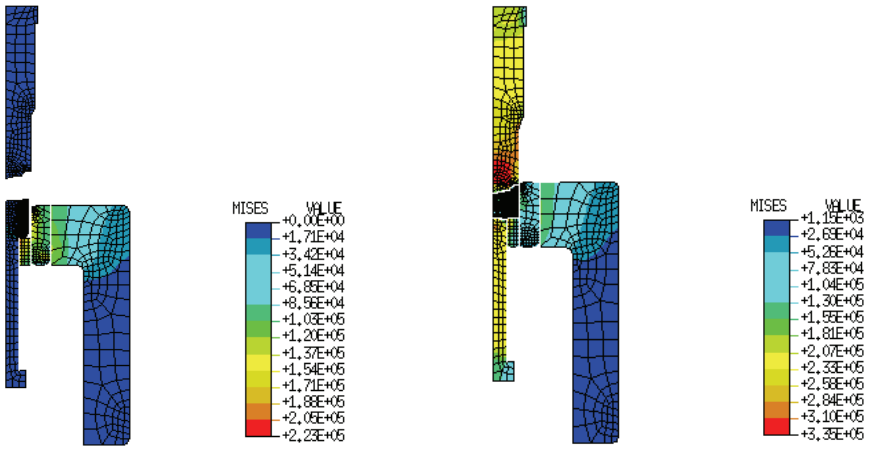

Figure 25: Von-mises stress contour in different steps of the 2nd stage forming (in Psi Maximum 2309.743 MPa)

the corner of the work piece slide along the master surfaces and cause penetration. This may be caused by the limitation of the contact algorithm. The solution is to use small sliding friction model in A/S and use high friction coefficient in A/E.

The fifth forming stage simulation

Mesh analysis in a rezoning problem in multi-stage forming subsequent stage:

Figure 26 illustrates the rezoning problem and the necessity for designing an appropriate intermediate initial mesh for a successful ALE formulation of subsequent stage in a multi-stage forming. Figure 26a illustrates the standard mesh rezoned after the end of stage 4. This mesh was not suitable for carrying out the last piercing operation using ALE algorithm. Hence a completely redesigned mesh suitable for successful simulation using ALE adaptive meshing in ABAQUS had to be constructed and is shown in figure 26b with equivalent plastic strain transferred to the new mesh. Even if we had numerical problems in simulating a good shape of the final chip produced during the piercing operation.

From Figures 27 and 28, we can see the Equivalent plastic strain contour at the onset of the fracture and when the piercing is finished. The position of the fracture initiation and the shape of the piercing edge and even the shape of the bur are also clearly shown.

Of course the precision of the shape of the piercing edge and the bur depend largely on the mesh and the parameters used in the fracture criteria.

Mesh refinement or complete rezoning at this time and material data from exper-

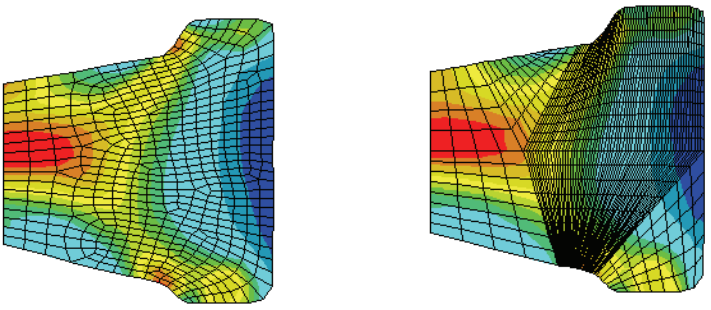

(a) before rezoning; (b)after rezoning

Figure 26: Mesh analysis in a rezoning problem to form the initial mesh for next stage adaptive meshing in multi-stage forming subsequent stage

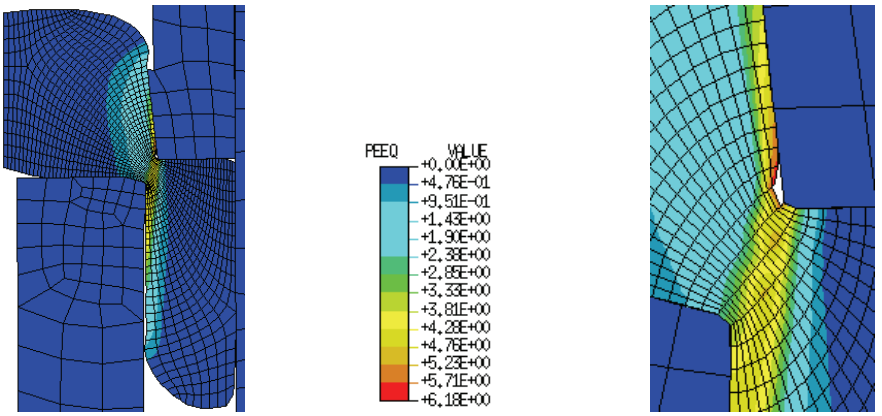

Figure 27: Equivalent plastic strain contour at the onset of the fracture

iment are needed for adjustment of material parameters and precise prediction of the final shape. There is element failure on the chip part. Even slower loading rate could not solve this problem, but as it occurs after the fracture initiation, it will not make a big difference on the final product.

Figure 29 shows the simulated load - displacement curve of the punch in the piercing stage. There is some noise after the fracture occurs. Analysis shows that this may be caused by the failure of the elements in the chip. We can clearly notice the softening effects in this picture.

The initial blank, the various semi finished products produced at various forming

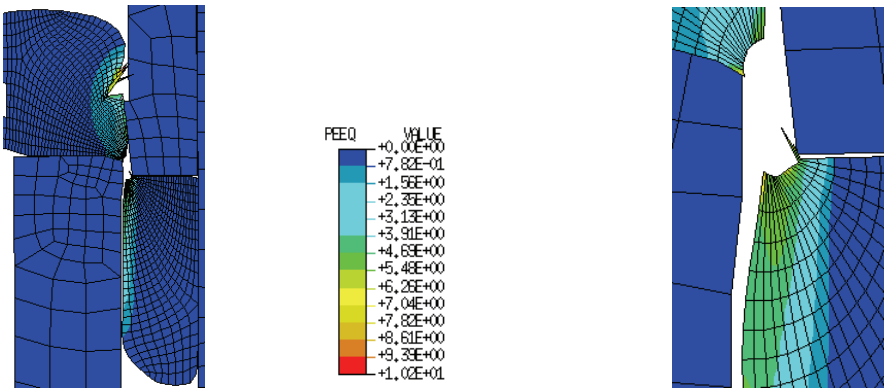

Figure 28: Equivalent plastic strain contour when the tearing complete

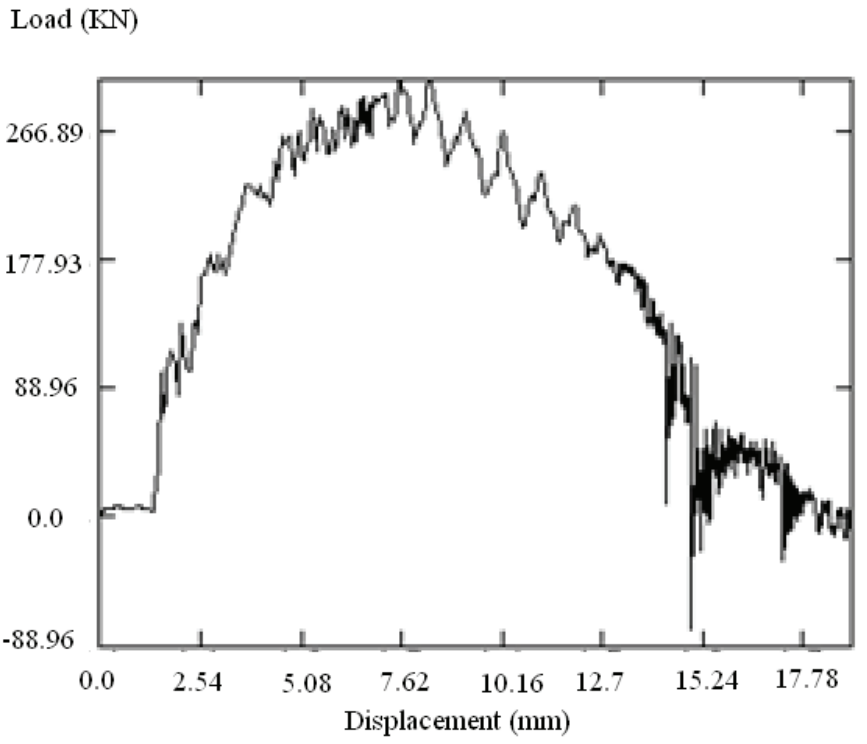

Figure 29: Simulated Punch load – displacement curve.

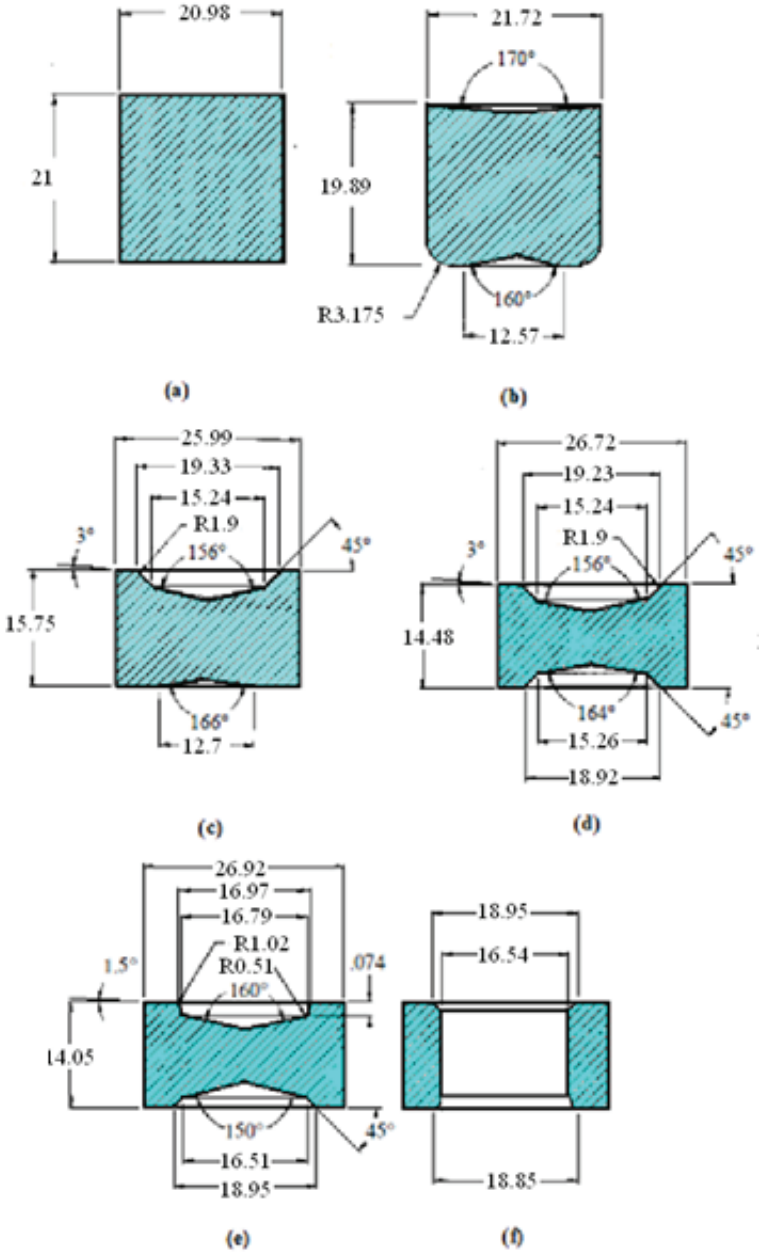

Figure 30: Intermediate semi-finished products and deformation sequence in various forming stages (values are in mm)

stages as well the final seamless ring are illustrated in figure 30.

In this example a physically based virtual manufacturing and process simulation methodology has been applied. The various forming stages are described as well as the analysis steps to be performed in ABAQUS are indicated for the complete process simulation analysis.

5 Conclusion and future work

When trying to apply the finite element simulation on whole workpiece- tooling process system in order to achieve a successful virtual metal forming operation, several technical problems should be addressed and solved before getting any reliable solution. In our approach, both the workpiece and the tools are deformable with contact and friction interactions between them. An integrated process simulation has been considered including preloading, such as shrink fits, multi-stage forming with both loading and unloading steps and from stage to stage. Adaptive meshing based on ALE formulation has been used and allowed to work with improved mesh quality preventing the analysis from terminating as a result of severe mesh distortion, thus providing faster, more accurate and more robust solutions than pure Lagrangian analyses.

All the stages and steps were simulated continuously so that the stress and deformation of the preceeding stages

and steps are taken as initial conditions of the following stages and steps. Hence stress and deformation effects are accumulated stage by stage just like in the real situation. In this way we can get the whole picture and complete information for the entire process, and realize to some extent of 'virtual manufacturing' dream.

Reliable results about spring backs, material damage and progressive failure of tools and workpiece and wall thickness distribution can be achieved from FEA, provided a good finite element model (including both appropriate element formulation and mesh size), good material laws (large strain plasticity, strain rate dependency, anisotropic yield and hardening function and appropriate damage and failure mode), good process parameters (part geometry, part-tool interaction, tool kinematics and dynamics) and appropriate loading paths are used. Most of the information is however process and material dependent so no universal set of parameters can be recommended. Experiments and further researches are thus needed for the determination of material parameters for fracture criteria.

One of the principal limitations of the finite element method in the solids mechanics problems involving large deformations is the remeshing problem, as a high-quality mesh must be maintained throughout the analysis. The ALE method makes it possible to solve efficiently such problems. The boundary representation of solid which

is based on ACIS is an adequate geometrical modeling which can be used in an ALE procedure. The ALE mesh can move independently of the material; however its topology, i.e. elements and connectivity, do not change during the adaptation and the solution variables on a deformed mesh are projected to the new mesh. However there are cases where a spatial initial mesh is needed to be able to benefit from ALE method, for example, in metal forming process involving large material flow. The pattern of such an initial mesh then depends on the flow pattern of the material.

For most problems, the ALE formulation reduces the cost of an analysis involving large deformations. Different smoothing approaches are adopted in this paper in order to remesh the computational domain without requiring the user intervention. This also eliminates manual rezoning for problems, where manual rezoning could be necessary. Remapping algorithms need to be evoked more frequently for the smoothing algorithm to be more efficient and for the advection to be more accurate. The purpose of the ALE formulation presented in this paper is to demonstrate that provided a good initial mesh is utilized, the ALE adaptive algorithms are able to provide updated mesh size and data that allow continuing the calculation beyond the point where the pure Lagrangian calculation fails. The considered examples problems demonstrate the effectiveness of ALE method in industrial application. The ALE methods presented in this paper have a wide range of applications and can be applied for fluid–structure problems arising from academia and industrial problems.

Further research and application works are needed to take into account of the thermal effects in cold forming process. These are the effects of heat generated by the deformation of the work material and by friction at the component-die interface, heat transfer from the component to the die, cooling of the component, die deflection due to temperature changes and the dimensional variation of the component resulting from thermal factors with different process conditions.

Acknowledgement: We gratefully acknowledge the support of NSERC strategic grant. We thank Lin Ying for performing most of the modeling and computational work with ABAQUS.

References

ACIS Spatial Corporation web cite at `http://www.spatial.com/products/acis.html`.

ASM (1969): *American Society of Metals, Metals Handbook,* Vol. 4 Forming, 8th edition, Metals Park, Ohio.

Aquelet N, Souli M, Olovsson L. (2006): Euler-Lagrange coupling with damp-

ing effects : Application to Slamming problems, *Computer Methods in Applied Mechanics and Engineering* v 195 Issue: 1-3 Pages: 110-132

Aquelet N, Souli M, Gabrys J, et al. (2003): A new ALE Formulation for Sloshing Analysis, *Structural Engineering and Mechanics* v 16 Issue: 4 p 423-440.

Askes H., Kuhl E., Steinmann P. (2004): An ALE formulation based on spatial and material settings of continuum mechanics. Part 2: Classification and applications, *Comput. Methods Appl. Mech. Engrg.* 193, pp 4223–4245

Altintas Y., Brecher C., Weck M., Witt S. (2005): Virtual Machine Tool, *CIRP Annals*, vol. 54 (22), p. 651-674, Elsevier.

Baaijens, F.P.T. (1993): An U-ALE formulation of 3D unsteady viscoelastic flow, *Int. J. Numer. Meth. Eng.* Vol. 36, p. 1115–1143.

Bathe KJ. (1996): *Finite Element Procedures,* Prentice-Hall: Englewood Cliffs, New Jersey.

Belytschko, T., Liu, W.K., Moran, B. (2000): *Nonlinear Finite Elements for Continua and Structures.* Wiley: New York.

Brokken, D., Brekelmans, W.A.M., Baaijens, F.P.T. (1998): Numerical modeling of the metal blanking process, *Journal of Materials Processing Technology*, v 83, 1998. p192-199.

Ceretti, E.; Taupin, E.; Altan, T. (1997): Simulation of metal flow and fracture applications in orthogonal cutting, blanking, and cold extrusion, *CIRP Annals - Manufacturing Technology*, v 46, n 1, p187-190.

Dvorkin, E.N., Petécz, E.G. (1993): An effective technique for modeling 2D metal forming processes using a Eulerian formulation, *Eng. Comput*, vol. 10 (4), p. 323–336.

Rugonyi S, Bathe KJ (2001): On finite element analysis of fluid flows fully coupled with structural interactions. *CMES: Computer Modeling In Engineering & Sciences*, Vol. 2, No. 2. pp. 195-212.

Groche P., Fritsche D., Tekkaya E.A., Allwood J.M., Hirt G., Neugebauer R. (2007): Incremental Bulk Metal Forming, *Annals of the CIRP,* vol. 56/2, p. 635-656.

Gurson, A. L. (1977): Continuum Theory of Ductile Rupture by Void Nucleation and Growth: Part I–Yield Criteria and Flow Rules for Porous Ductile Materials, *Journal of Engineering Materials and Technology*, vol. 99, p2-15.

Hallquist J.O. (2005): LS-DYNA Theoretical manual, Livermore Software Technology Corporation, Livermore (CA).

Pellet FL (2009): Contact between a Tunnel Lining and a Damage-Susceptible Viscoplastic Medium. *CMES: Computer Modeling In Engineering & Sciences* Vol. 52, No. 3, pp. 279-295.

Hamel V., Roelandt J.M., Gacel J.N., Schmit F. (2000): Finite element modeling of clinch forming with automatic remeshing, *Computers and structures,* vol. 77, p. 185-200

Hibbit, Karlsson and Sorenson Inc. (1998-2006): *ABAQUS Theory, Analysis and User's Manuals*, Version 5.8&6.6, Rhode Island.

Hughes, T., Liu, W., Zimmermann, T. (1981): Lagrangian–Eulerian finite element formulation for incompressible viscous flows, *Comput. Meth. Appl. Mech. Eng.* Vol. 29, p. 329–349.

Kim, H.-S.; Im, Y.-T.; Geiger, Manfred (1999: Prediction of ductile fracture in cold forging of aluminum alloy, *Journal of Manufacturing Science and Engineering, Transactions of the ASME*, v121, n3, 1999, p.336-344.

Lange, K. (1985): Handbook of Metal Forming, McGraw Hill Book Company, New York.

Lee, J.-H.; Kang, B.-S.; Lee, J.-H. (1996): Process design in multi-stage cold forging by the finite-element method, *Journal of Materials Processing Technology*, v58, n2-3, p174-183.

Longatte E, Bendjeddou Z, Souli M (2003): Application of Arbitrary Lagrange Euler formulations to flow-induced vibration problems, *Journal of Pressure Vessel Technology- Trans. of ASME,* v 125 Issue: 4,pp. p411-417.

Longatte E, Verreman V, Souli M (2009): Time marching for simulation of fluid-structure interaction problems , *Journal of Fluids and Structures* v 25, Issue: 1 pp. 95-111.

Pavana C. C.; Krishna Kumar, R. (1998): Remeshing issues in the finite element analysis of metal forming problems, *Journal of Materials Processing Technology,* vol. 75, p. 63-74.

Ponthot, J.P. (2002): Unified stress update algorithms for the numerical simulation of large deformation elasto-plastic and elasto-viscoplastic processes. *International Journal of Plasticity* 18 (1), 91–126.

Rekers, G. (1995): *Numerical simulation of unsteady viscoelastic flow of polymers*, Ph.D. Thesis, University of Twente.

Rachik M., Roelandt J.M. and Maillard A. (2002): Some phenomenological and computational aspects of sheet metal blanking simulation, *Journal of Materials Processing Technology*, vol. 128, p. 256-265

Rodrıguez-Ferran A., Perez-Foguet A., Huerta, A. (2002): Arbitrary Lagrangian–

Eulerian (ALE) formulation for hyperelastoplasticity, *Int. J. Numer. Methods Engrg.* 53, 1831–1851.

Saanouni, K. (2006): Virtual metal forming including the ductile damage occurrence: Actual state of the art and main perspectives, *J. of Materials Processing Technology* 177, 19–25.

Sharifi H. (1995): Maillage automatique par la méthode de quadtree/octree modifiée, Thàse présentée è la Faculté des études supérieures de l'Université Laval, Sainte-Foy, Québec.

Sheikh M.A. (2008): An assessment of recent developments in the finite element software for modeling manufacturing processes, *Int. J. Manufacturing Technology and Management*, Vol. 14, Nos. 3/4, p. 410-430.

Schreurs, P., Veldpaus, F., Brekelmans, W. Simulation of forming processes, using the arbitrary Eulerian–Lagrangian formulation, *Comput. Meth. Appl. Mech. Eng.* Vol. 58, p. 19–36.

Skov-Hansen, P.; Bay, N.; Gronbaek, J.; Brondsted, P. (1999): Fatigue in cold-forging dies: tool life analysis, *Journal of Materials Processing Technology* , vol. 95, Oct 15, p .40-48.

Zohouri S, Pirroz MD, Esmaeily A (2005): Predicting wave run-up using full ALE finite element approach considering moving boundary. *CMES: Computer Modeling In Engineering & Sciences*, Vol. 7, No. 1, pp. 107-118.

Stoker, H.C. (1999): Developments of the arbitrary Lagrangian–Eulerian method in non-linear solid mechanics, applications to forming processes, Ph.D. Thesis, University of Twente.

Tvergaard, V.; Needleman, A. (1982): Analysis of the cup-cone fracture in a round tensile bar, Acta. Metal., vol. 32, p157-169.

Van der Helm, P.N., Huétink, J., Akkerman, R. (1998): Comparison of artificial dissipation and limited flux schemes in arbitrary Lagrangian Eulerian finite element formulations, *Int. J. Numer. Meth. Eng.* Vol. 41 (6), p. 1057–1076.

Van Leer, B. (1977): Towards the ultimate conservative difference scheme. IV. A new approach to numerical convection, *Journal of Computational Physics* 23, p. 276-299.

Wisselink H.H., Huétink J. (2004): 3D FEM simulation of stationary metal forming processes with applications to slitting and rolling, *Journal of Materials Processing Technology* 148, 328–341

Yazdani, A., Gakwaya, A., Dhatt, G. (1999): éOn the post-processing techniques for elastoplastic axisymmetrical problems. *International Journal of Computational Mechanics,* vol.24, pp14-28.

Ying, L, Gakwaya, A., Guillot, M. (2003): The Application of finite element process simulation in cold forming, Laboratoire de CAO et Modélisation Mécanique, Dept de Génie Mécanique, Université Laval, (mémoire de maitrise 2003).

Zhu, Y.Y.; Zacharia, T.; Cescotto S. (1997): Application of fully automatic remeshing to complex metal-forming analyses, *Computers and Structures*, v 62, no 3, Feb, p417-427.